Copyright Warning & Restrictions

The copyright law of the United States (Title 17, United States Code) governs the making of photocopies or other reproductions of copyrighted material.

Under certain conditions specified in the law, libraries and archives are authorized to furnish a photocopy or other reproduction. One of these specified conditions is that the photocopy or reproduction is not to be "used for any purpose other than private study, scholarship, or research." If a, user makes a request for, or later uses, a photocopy or reproduction for purposes in excess of "fair use" that user may be liable for copyright infringement,

This institution reserves the right to refuse to accept a copying order if, in its judgment, fulfillment of the order would involve violation of copyright law.

Please Note: The author retains the copyright while the New Jersey Institute of Technology reserves the right to distribute this thesis or dissertation

Printing note: If you do not wish to print this page, then select "Pages from: first page # to: last page #" on the print dialog screen

ABSTRACT

MAPPING INTER-SUBJECT AND INTER-REGIONAL BRAIN CONNECTIVITY DURING FREE VIEWING OF NOVEL NATURAL SCENES

by
Sheela Nagaraj

Traditional functional magnetic resonance imaging (fMRI) studies have used controlled tasks such as finger tapping to isolate function in distinct cortical. Recent studies have examined the mechanisms involved during natural conditions by asking subjects to freely view the presentation of a movie. The objective of our study was to further observe the extent to which similarities are present between subjects during natural vision. It was hypothesized that there would be a linear relationship between the percentage of region-specific overlap, which is the percent of the anatomical region of interest which contains spatial activation exhibited by all six subjects, and corresponding temporal correlation values between subjects from those regions. In this study, a controlled experiment was conducted in which all the subjects viewed a movie clip from the 2005 thriller *Redeye* for the first time during the fMRI scan. Spatial and temporal correlations were examined during a forty minute movie clip in which subjects casually viewed the stimulus. Significant spatial overlap between the six scanned subjects was observed in many regions during the viewing of the forty minute stimulus and this overlap was considerably lower during the second ten minute viewing. Temporal correlation values as high as 0.8 were observed between subjects during the viewing of the forty minute clip. Inter-regional correlation was also examined within subjects. The use of a movie clip allowed for the activation of a numerous functional regions in a single duration to identify similarity in cortical activation during a complex stimulus both spatially and temporally.

MAPPING INTER-SUBJECT AND INTER-REGIONAL BRAIN CONNECTIVITY DURING FREE VIEWING OF NOVEL NATURAL SCENES

by
Sheela Nagaraj

A Thesis
Submitted to the Faculty of
New Jersey Institute of Technology
in Partial Fulfillment of the Requirements for the Degree of
Master of Science in Biomedical Engineering

Department of Biomedical Engineering

January 2008

APPROVAL PAGE

MAPPING INTER-SUBJECT AND INTER-REGIONAL BRAIN CONNECTIVITY DURING FREE VIEWING OF NOVEL NATURAL SCENES

Sheela Nagaraj

Dr. Sergei Adamovich, Thesis Co-Advisor — Date
Assistant Professor of Biomedical Engineering, NJIT

Dr. Bharat B. Biswal, Thesis Co-Advisor — Date
Associate Professor of Radiology, UMDNJ-NJMS

Dr. Tara L. Alvarez, Committee Member — Date
Associate Professor of Biomedical Engineering, NJIT

BIOGRAPHICAL SKETCH

Author: Sheela Nagaraj

Degree: Master of Science

Date: January 2008

Undergraduate and Graduate Education:

- Master of Science,
  New Jersey Institute of Technology, Newark, NJ, 2007

- Bachelor of Science
  New Jersey Institute of Technology, Newark, NJ, 2006

Major: Biomedical Engineering

Presentations and Publications:

Nagaraj S., Biswal BB. "Mapping Inter-Subject and Inter-Regional Brain Connectivity During Free Viewing of Novel Natural Scenes," NeuroImage October 2007 *Submitted*

Nagaraj S., Shah A., Shah P., Szeto V., Bergen M.T. "Ambulatory Preseizure Detection Device," Proceedings of the IEEE 32nd Annual Northeast Bioengineering Conference, Lafayette, 41;42, April 2006

To my beloved family and friends

ACKNOWLEDGMENT

I would like to express my deepest appreciation to Dr. Bharat B. Biswal, who served not only as my research supervisor, providing valuable and countless resources, but also constantly gave me support, encouragement, and reassurance. Special thanks are given to Dr. Sergei Adamovich, who has assisted me throughout the year provided me with valuable insight. Thanks are also given to Dr. Tara L. Alvarez for actively participating in my committee. I would also like to acknowledge Don Adams, Priyanka Bhatt, Parina Gandhi, Samata Kakkad, Sridhar S. Kannurpatti and Nirvish Shah for making the last year a memorable and enjoyable experience.

TABLE OF CONTENTS

LIST OF TABLES

Table **Page**

LIST OF FIGURES

CHAPTER 1

INTRODUCTION

1.1 Objective

The objective of this study was to investigate and develop novel methods in brain-mapping using functional Magnetic Resonance Imaging (fMRI) and study similarities in brain function within normal subjects. This procedure extends from research performed by Hasson et al. [1], in which cortical synchronization between subjects was observed during the casual viewing a movie. Conventional stimuli used in studying visual and auditory responses are generally very controlled (i.e., flashing checkerboard) however, by using a natural stimulus such as a movie the scenario created is quite similar to that which is experienced on a daily basis allowing one to understand cortical processing of natural vision and comprehension.

In this study, a controlled experiment was performed in which all the subjects viewed a movie clip for the first time during the fMRI scan. For additional control, the stimulus presented occurred entirely inside of an airplane and the scene focused on two individuals, therefore minimizing new visual inputs. Spatial and temporal correlations mediated by the stimulus were examined during a 40-minute movie clip, in which subjects were asked to casually view the stimulus. The first 10 minutes of the 40-minute clip were also presented for a second time to observe repeatability.

It is hypothesized that regions with significant overlap between the anatomical region and spatial activation mediated by the stimulus and observed in all subjects will

also result in a corresponding high inter-subject temporal correlation from that region. Specifically, we hypothesize that within regions that displayed significant region-specific overlap (RSO), a monotonic relationship between RSO and temporal correlation from the corresponding functional region exists.

1.2 Background Studies

From its development in the 1990's, functional magnetic resonance imaging (fMRI) has been used widely to understand human brain function in both healthy and patient populations. In 1991, Belliveau et al. [2] used regional cerebral blood volume (CBV) information in conjunction with the knowledge of hemodynamic and metabolic responses to construct the first functional magnetic resonance activation maps resulting from a visual task. The result was consistent with previous studies using Positron Emission Tomography (PET) imaging involving cortical observation, in which the stimulus produced increased activity in the primary visual cortex. Ogawa et al. [3] identified blood oxygenation level dependent (BOLD) fMRI to also measure detectable responses to visual stimuli in the primary visual cortex. Bandettini et al. [4] were one of the first groups to develop processing strategies for fMRI data sets by temporally correlating every voxel time series in the brain with an idealized reference waveform to detect corresponding local increases in the BOLD fMRI signal during the performance of particular task paradigms. Visual stimuli were used by Kwong et al. in 1992 [5] in addition to observing functional changes in humans during hand squeezing tasks and hypercapnia in animals.

In the last decade, attempts have been made to investigate cortical responses through the implementation of fMRI and allowed researchers to identify and distinguish between distinct functional regions in the cortex [6,7]. As a result, various scientific studies have provided significant evidence that despite the unique anatomy and processing ability of individuals, there is a remarkable inter-subject correlation between brain regions during specific tasks. These tasks usually consist of a simple stimulus aimed to target predicted responses as well as those that required the subject to endure fixation. For example, Tootell et al. [8] used controlled visual tasks to examine retinotopically categorized patterns within the cortex using fMRI. Using controlled studies, researchers have been able to identify different regions of the cortex, which are responsible not only for the overall visual experience but more distinct functions such as color, motion, and contrast. DeYoe et al. [9] used fMRI to compare visual fields between humans and macaque monkeys to identify and map the representation of the visual field in seven areas of the human cerebral cortex and to identify at least two additional visually responsive regions. Their results indicated that although there was considerable overlap between the human and macaque monkey visual field, the cortical organization may begin to differ in the extrastriate cortex beyond V3A and V4, which have shown to respond to orientation, spatial frequency, global motion, color and other detailed visual attributes.

fMRI has also proven to be a useful technique in observing abnormal functional activity in patients afflicted with various medical conditions and for pre-operative evaluation. fMRI is often used by surgeons to assess the degree to which a brain tumor may have shifted cortical regions surrounding the malignancy and consequently the

regions that can be removed without resulting in excessive harm to a patient's quality of life. This is accomplished by presenting a number of functional activation studies that would mediate activation in the corresponding functional regions adjacent to the tumor. "Functional MR imaging has a significant effect on therapeutic planning in patients with potentially resectable brain tumors and enables the selection of therapeutic options that might otherwise not have been considered because of functional risk," reported Jeffrey R. Petrella, M.D. and colleagues of Duke University, in the September 2006 issue of Radiology [10]. Pre-operative mapping and distinguishing between cortical regions during tasks is a key tool optimizing surgical removal of tumors. A study conducted by Hou et. al. [11] has indicated a significantly lower BOLD fMRI cerebral blood flow (CBF) response in brain tumor patients in comparison with healthy subjects thus, producing a lower response in a functioning cortical area. These changes in functionality due to malignant tumors may result in surgical removal of functioning regions presumed to be non-functioning. Additional imaging studies by Quarles et al. [12, 13] utilized fMRI parameters and the susceptibility to contrast to determine the characteristics of a tumor as well as its responses to therapy.

In another clinical study [14], two minimally conscious subjects (MCS) who were 18 months post-brain injury and at the verge of cognitive recovery were studied during a language paradigm using fMRI, PET and quantitave EEG. Results were compared to that of seven healthy controls. The paradigm consisted of various tasks including a personalized narrative spoken by a familiar voice and the time-revered version of the same narrative. Activation was considerable in language related areas such as the superior and middle temporal gyrus in both groups of subjects during the personalized

narrative task. During the time-reversed auditory stimulus, activation in the MCS patients was observed to be significantly reduced in comparison with the healthy controls indicating a decreased attention level during auditory stimulation with linguistically insignificant content. Tactile finger-tapping stimuli elicited bilateral responses of equal magnitude in both groups of subjects in the primary somatosensory area in the postcentral gyrus in corresponding hemispheres during the task. fMRI responses to the language related tasks were compared to results attained from FDG-PET and EEG and indicated a lower than normal global resting metabolic rate in MCS patients as well as differences between the normal and MCS subjects in the metabolic resting rates for each hemisphere and baseline activity. Abnormal metabolic rates in patients in the persistently vegetative state were observed in a study by Schiff et al. in 2002 [15] where PET and fMRI analysis indicated a 30%-40% decrease in overall cerebral metabolism in comparison to normal subjects. Several isolated cortical regions also demonstrated metabolic rates considerably higher than normal and demonstrated a reduction of evoked responses and neuronal firing. Also, a decrease in inter-regional correlation within the injured hemisphere indicates decreased capabilities of functional integration in MCS subjects. It can be predicted that understanding the functional mechanisms corresponding to the minimally conscious state will provide guidance into rehabilitation strategies to offer patients with the most excellent quality of life possible. A possible therapeutic application in rehabilitating those in the minimally conscious state [16] is suggested to be deep brain stimulation (DBS) in areas that were shown to be less reactive to stimuli in functional imaging studies.

Recognizing the unique functional differences between various clinical populations with neurologically related abnormalities will play an important part in assessing the cognition and functionality of these patients although they may not be apparent, and potentially provide them with an opportunity for full functional recovery.

Although controlled studies provide insight into brain function, natural vision cannot be accurately modeled through these conventional methods due to its complicated structure. Characteristics of natural vision include components which are embedded within a dynamic, complex scene, no necessity for fixation, and often times visual cues are associated with other components such as context or emotion [1]. Recently, Hasson et al. [1] utilized a novel method of presenting natural sequences to observe responses from subjects during the free viewing of a 30-minute clip from the movie "The Good, the Bad and the Ugly (1966)". On average they found that during the viewing of the movie there was a 29% ± 10 inter-subject overlap in spatial activation which covered not only the audiovisual sensory regions but additional somatosensory areas. The study also indicated similarities between subjects where there was an increase in temporal activity in particular regions which corresponded directly to the components presented within the stimulus such as faces, buildings, and hand gestures.

Bartels and Zeki [17], presented the first 22 minutes of the James Bond movie "Tomorrow Never Dies" to subjects during the acquisition of fMRI images to understand neural processing during natural vision. Subjects were asked to perceptually rate the intensity of their visual experience based upon specific criteria such as colors, faces, language and bodies. The subjective responses were convolved with the hemodynamic response function and correlated to the fMRI BOLD activity from various regions within

the brain mediated by the presentation of the movie. Results indicated that despite the complexly integrated nature of the stimulus, functional segregation was present and observed, as each element correlated with its corresponding cortical region. Colors, faces, language and bodies corresponded to activation in V4, fusiform gyrus, Wernicke's Area and the superior temporal cortex, respectively. Considerable inter-subject temporal correlation was also seen between the subjects in the four distinct regions.

In a different study, Bartels et al. [18] hypothesized that the utilization of a natural stimulus allows for a novel way of constructing activation maps based on the correlation of BOLD signals between functional regions. fMRI was used to attain cortical activity data as subjects freely viewed a movie clip with intermittent rest periods. Independent Component Analysis (ICA) was used to separate signals based on BOLD dynamics. It was concluded that during the viewing of the natural stimulus, correlation between regions that were anatomically connected were considerably higher than between unconnected regions and functional specificity within regions increased during natural viewing in comparison to resting conditions. The authors hypothesized that these changes between baseline and active states may provide insight into cortical connectivity during relatively natural conditions.

To observe cortical functionality in natural settings, Malinen et al. [19] performed fMRI on six subjects during 8-minute blocks of unpredictable auditory, visual, and tactile finger tapping stimuli. Independent component analysis (ICA) and general-linear-model-based analysis (GLM) were compared and used to identify significant components in the brain. It was found that a significant component was found in the superior temporal sulcus that reacted to auditory stimuli. Further analysis indicated various visual regions

that responded to visual stimuli and others that further discriminated between visual objects in the presented stimuli (i.e., buildings, faces).

fMRI studies have introduced many possibilities of using the intrinsic blood-tissue contrast basis of nuclear magnetic resonance to understand the spatial and temporal aspects of brain function. fMRI scanning has permitted researchers to identify and map changes related to perceptual, motor and cognitive function by relating metabolic and hemodynamic changes during a particular task. fMRI has many benefits including increased spatial and temporal resolution, in addition to being non-invasive in comparison with alternative imaging modalities making it a useful tool in examining cortical functionality. Spatial comparison denotes the capability to discriminate changes across different spatial locations while temporal comparison refers to changes within the same region over time. The spatial resolution can be further enhanced by sacrificing coverage, increasing the scan time or by using higher field-strength magnets to increase in signal-to-noise ratio (SNR). Prior to the popular use of fMRI as a functional neuro-imaging tool, the most accepted modality was positron emission tomography (PET) which requires the injection of radioactive tracers to quantify variations in the brain through parameters such as glucose metabolism and blood flow. Although PET was a powerful tool in understanding cortical functionality, there were numerous disadvantages such as the invasive procedure which required the injection of radioactive tracers, expenses of developing the radioactive isotopes and the sluggish image acquisition rate. In comparison to fMRI, the spatial resolution of PET data sets is quite limited. The temporal resolution of fMRI is several times better than the 30-45 sec of PET and further, by decreasing the area of coverage, the number images that can be acquired per second

can be increased. The technological advances in fMRI have significantly increased awareness of functional neuro-imaging studies over the last ten years and the clinical and research applications of this imaging modality are countless.

This Master of Science thesis utilizes fMRI to investigate the extent of spatial and temporal inter-subject synchronization during a complex stimulus using multiple analysis methodologies. Following the background studies described previously in Chapter 1, Chapter 2 presents the fundamentals of functional magnetic resonance imaging including a description of the scientific principles behind the generation of the fMRI signal, as well as the biological properties represented in the signal. Chapter 3 provides a detailed outline of the investigational study performed for this thesis and an interpretation of the results obtained. Chapter 4 concludes the work presented and offers thoughts on future applications.

CHAPTER 2

FUNDAMENTALS OF FUNCTIONAL MAGNETIC RESONANCE IMAGING

2.1 Foundations of Nuclear Magnetic Resonance

Studies surrounding the nuclear magnetic resonance signal initiated during the 1940's in an attempt to uncover applications in chemistry and biochemistry. During the late 1960's, it was identified that water molecules, regardless of whether or not they were present in living tissue, could be imaged using nuclear magnetic resonance techniques. In the 1970's, American chemist Paul Lauterbur (whose joint work with Peter Mansfield in the development of magnetic resonance imaging (MRI) awarded him the Nobel Prize in Physiology/Medicine in 2003) manipulated the magnetic field gradients to localize the magnetic resonance signal in space and generate an image. Clinical applications were identified in the mid-1980's giving way to what is known today as magnetic resonance imaging (MRI). The development of MRI provided researchers and clinicians with major advantages over existing imaging modalities including its non-invasive procedure, excellent resolution in both bones and soft tissue as well as the ability to attain images through any plane within the body. The basis of the formation of the MR signal can be summarized through a series of physical principles. Understanding the magnetic properties of the atom is fundamental in comprehending the generation of the magnetic resonance signal.

Many biologically abundant elements are capable of producing magnetic resonance images, hydrogen being the most plentiful and magnetic. Water content is

largely present throughout the human body and accounts for 70.6% of gray matter within the brain, 84.3% of white matter in the brain, 12.2% of bone, 93% of blood and 80.3% of the heart. Protons of these elements can be modeled as an extremely small bar magnet with poles on either end, as seen in Figure 2.1. A fundamental theory is that of the nuclear spin, in which atomic nuclei that possess a magnetic moment and angular momentum (denoted as spins) demonstrate fast gyroscopic precession when placed in an external magnetic field. The axis about which the spins precess is known as the longitudinal direction while the plane in which precession occurs is known as the transverse plane. In the presence of a strong magnetic field, the spins of the protons within the material are arranged in two energy states. The lower state is parallel to the

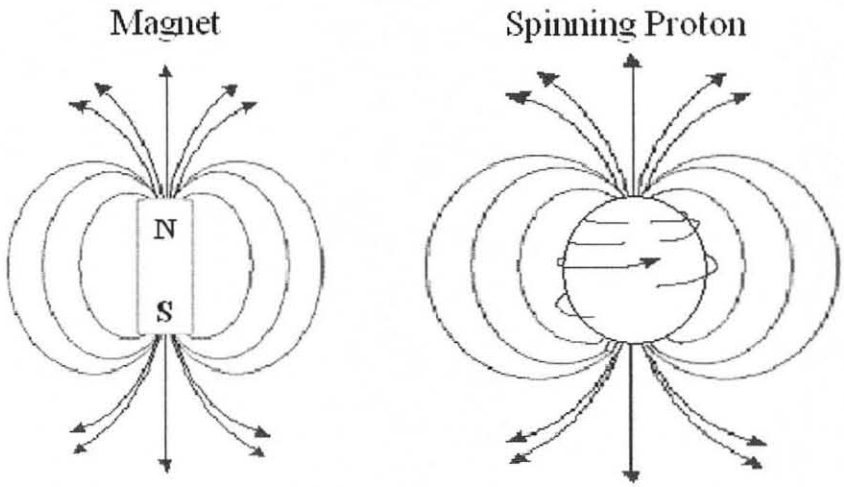

Figure 2.1 Comparison of bar magnet and proton.

applied magnetic field and the higher state is anti-parallel to the magnetic field. The energy difference between both states is proportional to the strength of the magnetic field. Within the two energy levels, the protons precess at an angular frequency dependant upon the strength of the magnetic field. The relationship between magnetic field strength and precessional frequency is given below in Equation 2.1 by the Larmor equation, where ω_0

is the precessional angular frequency, γ is the gyromagnetic ratio which is dependant upon the element and gives the proportionality constant between the magnetic moment and the angular momentum, and B_0 is the strength of the magnetic field. For fMRI, the strength of the magnetic field used is usually between 1.5 to 4.0 Tesla with greater strengths for research applications.

$$\omega_0 = \gamma B_0 \tag{2.1}$$

As the protons precess based upon their orientation in the parallel and anti-parallel directions, there is no net magnetic field at equilibrium due to the random circulation of protons. As energy is applied in the form of radiofrequency electromagnetic radiation at the particular precessional frequency proportional to the energy difference between the two states, (also known as the Larmor frequency) the energy is absorbed and more spins are converted from the lower to the higher energy anti-parallel state. After the applied energy is absorbed, the system attempts to reach equilibrium once more, resulting in the release of the magnetic resonance signal. During equilibrium, more spins are in the parallel (low energy) state causing a maximal longitudinal magnetization. As the energy is applied to the system (Figure 2.2), there is a gradual increase of the protons in the high

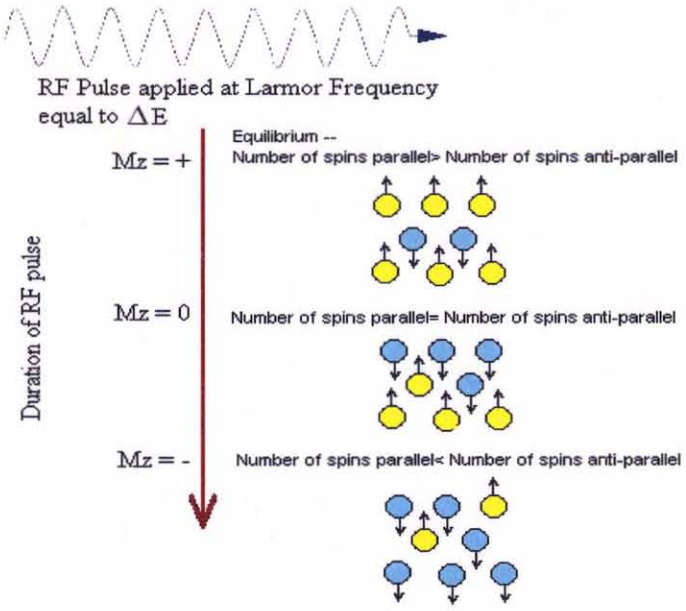

Figure 2.2 Quantum mechanics description of changes in longitudinal magnetization and proton spin orientations due to application of RF waves at Larmor frequency.

energy state causing a maximal decrease in longitudinal magnetization (along the z-axis). To measure this variation in magnetization, it is necessary to displace it to the transverse plane (the x-y plane) from its perpendicular position in respect to the magnetic field and thus quantify the changes within the magnetic flux. To do so, a 90-degree RF pulse is used, resulting in the largest transverse magnetization possible [21].

2.2 T1 & T2 Parameters

As a 90-degree RF pulse is applied, it results in a phase coherence of protons causing a maximal transverse magnetization in the sample. As this magnetization precesses at the Larmor frequency, the protons dephase producing an electronic signal which can be represented as a damped sinusoid called Free Induction Decay (FID). Internal (spin-spin interactions) and external (inhomogeneities in the magnetic field) cause the damping to occur even faster. T2 represents an exponential relaxation time (between peak transverse

signal and 37% of the peak level) due to the intrinsic properties for the given sample. If the extrinsic properties are also considered (such as irregularities in the magnetic field), the loss of coherence occurs much more rapidly and therefore the T2 time is shortened to T2*. The value of T2 is influenced by the structure of the sample for example, T2 in amorphous fluids is long because the rapid motion of the molecules allows for the intrinsic homogeneities to be negligible. Also as the size of the molecule increases T2 becomes shorter due to the restriction of their motion. The relationship between T2 and transverse magnetization following an RF pulse can be described by Equation 2.2:

$$M_{xy}(t)=M_0e^{-t/T2} \tag{2.2}$$

T2 decay occurs at a much quicker speed in comparison with T1, which is the return from excited magnetization ($M_z = 0$) to the equilibrium (M_0), maximum longitudinal magnetization. T1 relaxation is longer than T2 because the excited protons must discharge their energy into the surrounding tissue lattice, depending upon the spin-lattice characteristics for interaction. The T1 constant is the time needed to improve to 63% of the maximum longitudinal relaxation after a 90-degree RF pulse has been applied. T1 depends on various factors including the energy absorbed by surrounding tissue, the structure of the surrounding lattice, and directly to the strength of the magnetic field. Longitudinal magnetization is described by the following given in Equation 2.3:

$$M_z(t)=M_0\,(1-e^{-t/T1}) \tag{2.3}$$

Figure 2.3 illustrates the changes corresponding to the properties of transverse and longitudinal magnetization.

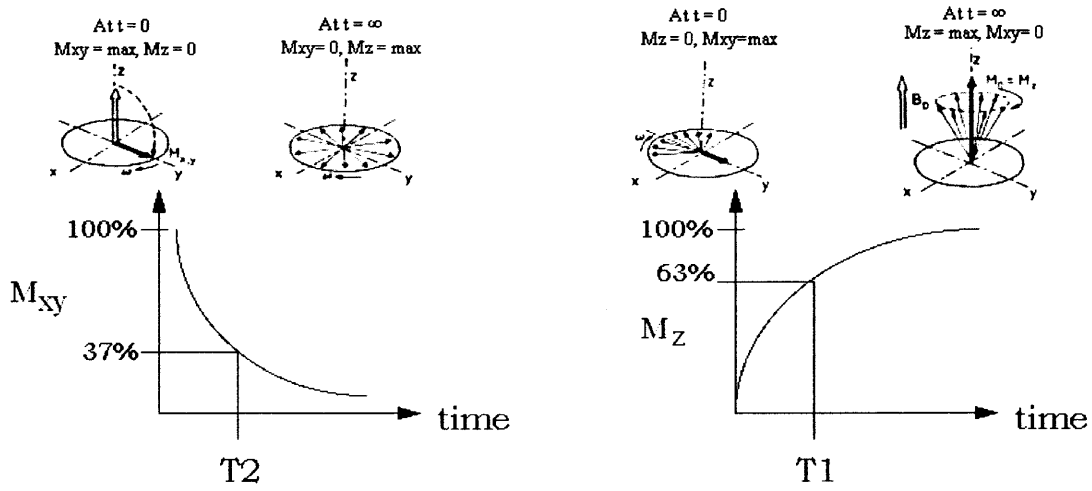

Figure 2.3 Comparison of T1 and T2 relaxation parameters. During the initial time after the RF pulse is applied, transverse magnetization is at a maximum and longitudinal magnetization is at zero. As time progresses, transverse magnetization decreases causing a maximal longitudinal magnetization.
(Source: http://wbs-med.imib.rwth-aachen.de/cbt/Radiologie/Skript/allgemein/relax4.gif)

After the application of the radiofrequency energy, the changes in the magnitude of the transverse magnetization vector can be quantified over time allowing for the measurement of the MR signal through the external detector coil. The Bloch equation (provided in Equation 2.4) provides a quantitative summation of the magnetic resonance phenomena described. The Block equation describes how the net magnetization of a spin system varies over time when exposed to a time varying magnetic field:

$$\frac{dM}{dt} = \gamma M \times B + \frac{1}{T_1}(M_0 - M_z) - \frac{1}{T_2}(M_x + M_y) \tag{2.4}$$

Where dM indicates the change in net magnetization, dt is the change in time, γ is the gyromagnetic ratio, M is the net magnetization, B is the total magnetic field experienced by the spin system, T_1 is the constant that expresses the longitudinal component of the net magnetization over time, M_0 is the initial magnetization, M_x, M_y and M_z are the net magnetizations in the x, y, and z directions, respectively and T2 is the

time constant that describes the decay of the transverse component of the net magnetization over time.

T1 is quite longer than T2 and factors that effect the values of T1 and T2 include molecular motion, size and interactions. For example, within a soft tissue, T1 is usually around 500 msec and a T2 value about 5 to 10 times shorter. The variations in T1, T2 and T2* values are responsible for the high resolution in MRI, which allows it be a non-invasive diagnostic tool. All molecules can be categorized into three categories: small sized moving at fast speeds, medium sized with medium speeds and large slow molecules. Small molecules tend to have long T1 and T2 values, medium sized molecules have short T1 and T2 values and large slow molecules have long T1 and short T2 times. A majority of the molecules being imaged within the body have a tendency to be small to medium in size. T1 values are also heavily influenced by the strength of the magnetic field while there are negligible effects on the T2 value. In addition, another constant parameter that defines the contrast of the acquired images is proton density within the material being imaged. Variations in these contrast parameters based on the characteristics of tissue create a measured signal which is specific to the type of tissue being observed.

Since the 1990's, as fMRI studies became prominent, there has been an emphasis on T2* weighted images due to the importance of BOLD contrast. A majority of fMRI studies currently utilize T2*-weighted pulse images. A schematic of the pulse sequence often used for T2* weighted images is given in Figure 2.4. T2* weighted images are

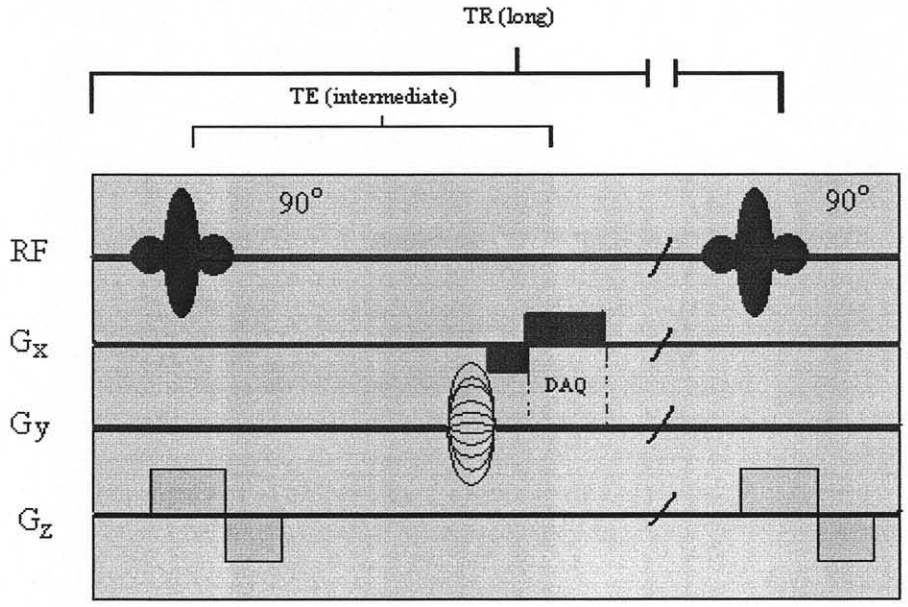

Figure 2.4 Pulse sequence used for T_2^*-weighted images, most commonly used for BOLD-contrast fMRI due to sensitivity of deoxygenated hemoglobin level.

especially sensitive to the quantity of deoxygenated hemoglobin present within a tissue and susceptible to minor variations in the BOLD signal which correspond to metabolic activity. T2* contrast is emphasized by influencing pulse sequences (see Section 2.4) to have a long TR and medium TE value. By doing so, there is an increase in the field homogeneity which is a major factor that effects the T2* parameter [21].

2.3 Localization of the Magnetic Resonance Signal

When protons in a material are exposed to an external magnetic field and specific radio frequency waves are applied, they result in the release of signals dependant upon the excitation and relaxation attributes of that material. An essential concept in understanding MR imaging involves the use of additional magnetic gradients imposed upon a uniform magnetic field to allow for spatial localization within the subject.

Uniform magnetic fields are produced in a coil wire and supplied with energy through a specified direct electric current. Magnetic field gradients are created by overlaying the magnetic fields with coils in a particular configuration to create a field that varies in strength linearly proportional to distance along the magnetic field. The surroundings of the magnet bore contain gradients along the x, y and z directions and each result in a linear change in corresponding precessional frequency of protons based upon their spatial location relative to the null frequency, a reference point which causes no net change in the magnetic field. Protons present in a particular location are identified by their spatial location within magnetic field and the unique strength of the field at that region created by the configuration of gradients.

When radiofrequency waves are applied at a particular precessional frequency, there is a change in the magnetic moment that occurs within the tissue causing the orientation of residing protons to deviate from the equilibrium state to the anti-parallel orientation. As the protons return to the equilibrium state, MR signals can be detected based upon the amount of excited protons in a particular region of the tissue.

The function of the RF coil is to produce RF pulses that are used in conjunction with the slice select gradient (SSG) in MRI to identify the particular slice within the body that needs to imaged and excite those regions by turning RF coils on and off specified to the Larmor frequency corresponding to that area. The gradient used in slice selection creates a net positive and negative magnetic surrounding that adds and subtracts from the main magnetic field (Figure 2.5). Due to this change in the field, corresponding precession frequencies are also altered based upon their location within the gradient

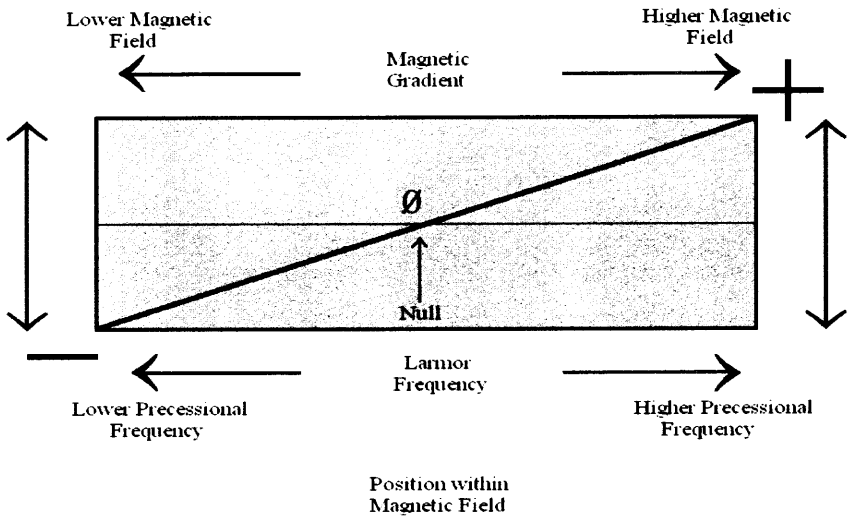

Figure 2.5 The gradient magnetic field generates a net magnetic field that alters the main magnetic field in a positive and negative way depending upon the position within the field of view. The proportional difference in magnetic field over distance results in a proportional change in corresponding precessional frequencies.

proportional to the magnetic field strength at that region. The specific RF pulse is utilized to activate a particular rectangular slice of protons in the sample using a "sinc" pulse. This function is used because it is focused at a center point at time zero as well as positive and negative oscillations that decrease in amplitude prior to and following the peak. To attain a perfect rectangular slice, it is necessary to generate an exact sinc pulse that has an infinite period of time before and after the pulse, which is not practically feasible. Because short pulses cause a cutoff of the sinc function, longer RF pulses provide better slices. The width of the sinc pulse identifies the corresponding bandwidth of the slice so a large pulse width corresponds to a wide band width. It is however better to have a narrow bandwidth to improve the signal to noise ratio conversely, signal to noise ratio is also improved when in the presence of a higher external magnetic field.

The second component used for spatial identification is the phase encode gradient along the y axis for axial images. Following the application of the slice selection gradient,

all spins within that particular region of tissue have coherence of phase. As the phase encode gradient is activated a linear change in precessional frequency occurs along the slice in the direction of the newly introduced gradient. Subsequent to the phase encode gradient being turned off, all precessions go back to the Larmor frequency however, all spins differ in phase with protons toward the positive pole undergoing a forward phase shift and the backward shifts to those toward the negative pole. The degree of the phase shift is based upon the spatial location with respect to null frequency region, as well as the strength of the strength of the phase encode gradient field. The final component in spatial encoding is the frequency encode gradient. As the name implies, the frequency encode gradient is applied to spatially determine tissues based upon the resonant frequency which is slightly higher on tissues toward the positive pole relative to those near the negative pole. Frequency encoding allows for spatial localization in the x-direction only [21].

2.4 Pulse Sequences

When acquiring anatomical images of the brain, it is more valuable to have excellent contrast, and acquisition speed can be sacrificed due to the static nature of the images. In functional imaging, it is necessary to study changes occurring in cortical activity and therefore in addition to the spatial resolution, temporal resolution and the speed of acquisition are also a significant consideration. Various pulse sequence techniques have been developed for functional imaging that have the ability to acquire rapidly a series of images with minimal distortions in a relatively short period of time. Various pulse sequences can be implemented to acquire images that are sensitive particularly to tumors,

blood vessel abnormalities, bone damage, and multiple other conditions. This allows fMRI to be prevailing tool in clinical and research studies.

The concept of *spin echo* is used to conceptualize the initial excitation of magnetized protons by using an RF pulse to create free induction decay. After the application of the first 90-degree RF pulse which relaxes according to the T2 or T2* parameter, a second 180-degree pulse is used to re-establish phase coherence and thus an echo. By manipulating the timing between the pulses there is an ability to control contrast properties within the tissue. During the *time of echo* (TE) there is a re-phasing of spins and therefore a signal can be measured. The 90-degree pulses are separated by a *time of repetition* or TR.

Echo planar imaging (EPI) was developed by British physicist Peter Mansfield and colleagues of the University of Nottingham. Mansfield was recognized for his contribution to Medicine with the Nobel Prize in Physiology in 2003 (in collaboration with Peter Lauterbur). In this technique the whole *k*-space is filled by altering the gradients quickly after an excitation. This concept, along with technological developments in gradients that allowed for the rapid switching of gradients, has caused EPI to become the most commonly used imaging technique in fMRI. In this method, all data is acquired before considerable T2 (or T2*) decay occurred and the *k*-space is filled after one excitation. In magnetic resonance imaging, the *k*-space is the area where raw data from acquired images are temporarily stored after they have been digitized. After the *k*-space is filled at the end of the acquisition, the data is processed using mathematical algorithms to create a final reconstructed image. The *k*-space is denoted in the spatial frequency domain and defined using frequency encoding, phase encoding and other

related parameters. Regardless of how complex the structure is of a particular image is, it can be represented through a pattern of spatial-frequency components. The k-space contains all information about the attained images including signal to noise properties, contrast and resolution. Each line within the *k*-space is filled with raw data for each interval of pulse repetition time. In EPI, the *k*-space is filled quite rapidly to ensure sufficient spatial resolution making it essential to have a strong magnetic gradient configuration for switching. In EPI, the *k*-space is filled by alternating in lines from opposite directions opposed to the conventional spiral method. This switching action of gradients is dependant on the hardware of the gradients as it is vital that the gradients create 90-degree turns for the pattern used in filling the k-space (Figure 2.6). Echo-planar images have been used to acquire as quickly as 64 per second in a single slice or from the entire brain at about four per second [22].

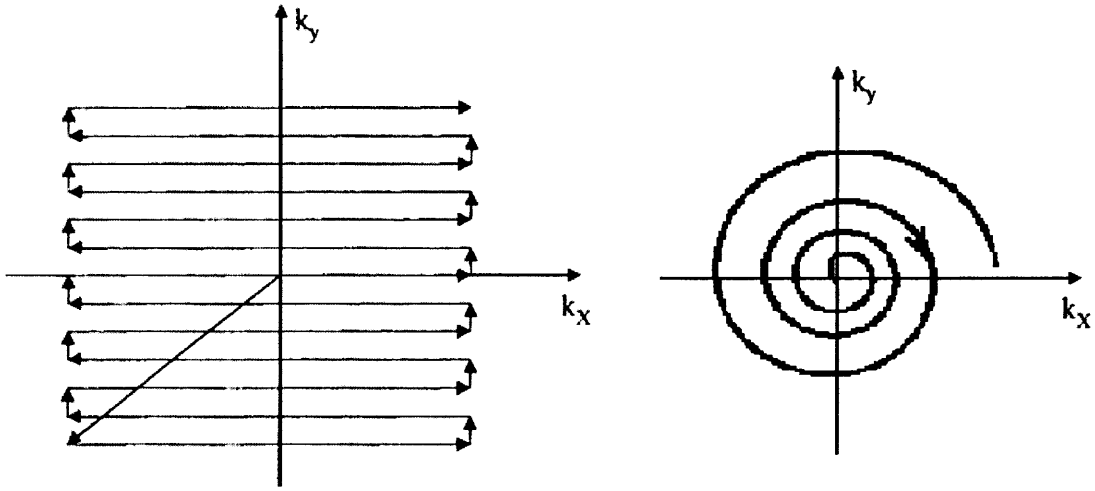

Figure 2.6 Echo Planar Imaging acquisition (left) and Spiral Acquisition (right). As can be seen, the direction of the gradients used in EPI acquisition must be changed very quickly to allow the direction change through the k-space.
(Source: www.scielo.br, www.urmc.rochester.edu)

2.5 Introduction to Neuro-anatomy

It is important to understand the anatomical structures within the brain and their functions to efficiently assess the results of functional neuro-imaging studies. This section will provide a basic introduction to neuro-anatomy and key functional regions addressed in this study.

The central nervous system or CNS consists of the brain and the spinal cord. The CNS can be considered a long cylindrical entity which extends from the tailbone to the skull and bends at a 90-degree angle towards the nose where it enters the brain. The CNS is made up of various cellular components such as neurons, the basic processing unit in the nervous system (Figure 2.7). The body of the neuronal cell is called the *soma* and it

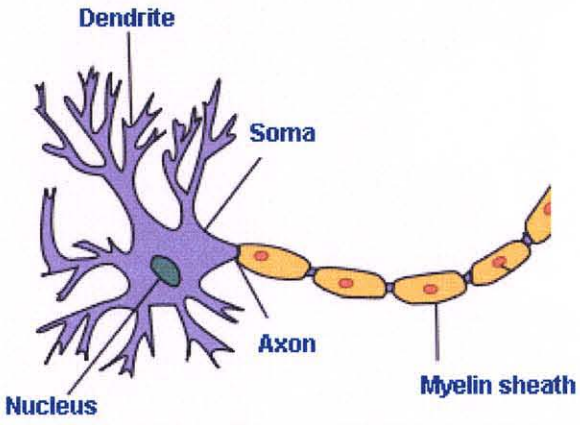

Figure 2.7 Drawing of a neuron.
(Source: http://en.wikipedia.org/wiki/Image:Neuron-no_labels.png)

contains the cytoplasm, the cell nucleus and organelles. *Dendrites* which are located on the neuron attain signals from other cells and integrate information while the neuronal *axons* transmit signals through electrical pulses from the cell body to the junction between neurons known as the *synapse*. Neurotransmitters are also released by pre-synaptic neurons over this junction to influence receptors on post-synaptic neurons. Neuronal activity is dependant upon membranes consisting of lipid bi-layers. These

membranes restrict chemical flow into the neuron through passive concentration gradients and pumps restricted by molecular and electrical potential differences. There are two major types of neurons, pyramidal cells and stellate cells. Pyramidal cells have a triangular cell body shape and long axons which can extend large distances while stellate cells have a more spherical shape and assist in processing. A majority of the CNS is composed of cell bodies called gray matter and as well as a portion called white matter which is composed of axon bundles made of a fatty myelin sheath which increases conduction speed of action potentials. The myelin sheath is created through the assistance of two types of support cells (collectively known as *glial* cells) called *oligodendrocytes* and *astrocytes*.

There are three membranes (known as *meninges*) over the cortical surface. The outmost region is the thick and tough *dura* followed by the web-like *arachnoid* layer and the inmost, delicate *pia* layer. The pia is high in vasculature and is composed of many small arteries that supply blood to the brain. The region between the arachnoid and pia is packed with cerebrospinal fluid (CSF) a clear liquid which lubricates the brain and spinal cord. CSF flows into the ventricles of the brain filling the cavities in the brain, though additional ventricles and brain stem in both directions and eventually is absorbed into the vascular system. CSF creates a cushion that shelters the brain from its thick and bony outer layer in addition to maintaining a constant environment to harbor the brain and assist in maintaining metabolic wastes.

The spinal cord enters into the brain through an opening at the bottom of the skull known as the *foramen magnum*. It extends and connects sensory fiber tracts within the body to transmit somatosensory information from the brain to control muscles. Rostral

(towards the front of the brain) to the foramen magnum is an extension of the spinal cord known as the *medulla oblongata* which contains major cranial nerves and serves a purpose in respiration control, circulation and other autonomic functions. The structure known as the *pons* is located rostral to the medulla and plays a similar role as well as controlling additional cranial nerves involved in managing facial and eye muscles. Posterior to the pons is the *cerebellum*, a large entity which is significant in coordination of walking and posture, motor learning and similar functions. Rostral to the pons is the *mid-brain* that two major cranial nerves and numerous other important structures initiate from. The collective unit which includes the mid-brain, pons, and medulla is called the brain stem. Rostral to the mid-brain is the hypothalamus, responsible for temperature and endocrine function regulation, water intake, and hunger. The adjacent thalamus receives sensory, motor, and other information and organizes and projects it into corresponding regions of the brain.

The *cerebrum* or brain is essentially an unbroken sheet of cerebral cortex which has been creased into a mold of peaks and troughs within the cortical surface known as gyri and sulci, respectively (see Figure 2.8). If the average human cortex was unfolded

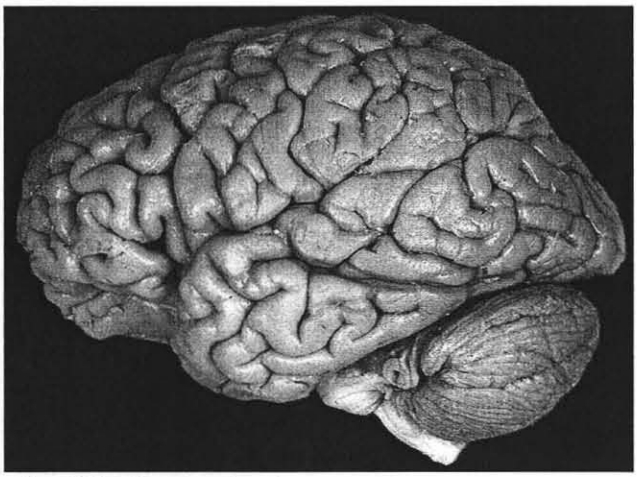

Figure 2.8 Photograph of the human brain.
(Source: http://www.muskingum.edu/~psych/psycweb/gifs/brainpic.gif)

and laid out as a sheet it would have the area of 2500 cm^2. The cerebrum can be divided into four main lobes based upon functionality and location. The hemispheres are separated by the longitudinal fissure and the temporal lobe is separated from the frontal and parietal lobes by the Sylvian fissure. As its name infers, the frontal lobe is located in the front of the cerebrum. It is positioned anterior to the parietal lobe and above the temporal lobe. Many key regions that assist in voluntary movement are located within the frontal lobe including the *precentral gyrus* and *central sulcus.* This region, which is responsible for movement, is jointly known as the *primary motor cortex.* The frontal lobe has also been attributed to impulse management, judgment, language production and comprehension (*Broca's Area*), working memory, motor function, and socialization skills. It is especially important in defining ones character and behavior as well as assessment of consequences of action (*Orbitofrontal cortex).*

The temporal lobe is located on the sides of the human cortex and beneath the lateral (Sylvian) fissure. Its purpose is auditory processing and it encases the *primary auditory cortex.* The region within the temporal lobe known as the *superior temporal gyrus* contains the primary auditory cortex where auditory information from the *cochlea* is sent for processing. Another prominent area, known as *Wernicke's Area* is located in the temporal and parietal lobes and along with Broca's Area it plays a role in language comprehension and memory control. Additional functions in the temporal lobe include high level visual processing in regions such as the *fusiform gyrus* for face recognition and the parahippocampal gyrus for recognition of scenes. Some anterior temporal regions are involved in perception and recognition of objects (*inferior temporal gyrus*).

The parietal lobe is situated superior to the occipital lobe and posterior to the frontal lobe. The parietal lobe serves as an integrator of sensory information and provides assistance in determining surroundings and navigation. Within the parietal lobe the *postcentral gyrus* contains the primary somatosensory cortex which is the key sensory reception and integration site. It also contains the *precuneus*, a part of the limbic system which studies have shown contributes to emotional and memory management. The structure known as the *angular gyrus* has shown to be related to language and cognition and the *supramarginal gyrus* has been known to show activity during tasks involving somatosensory information and motor tasks involving sensory feedback.

The occipital lobe is the visual processing center of the mammalian brain. It is located on the back-most part of the cerebrum and is part of the forebrain area. Retinal sensors transmit information from visual stimuli through optic tracts. The cortex receives this information from the outer half of the retina on the same side of the head and the inside half of the retina on the opposite side of the head. The *primary visual cortex* (V1) is located on the posterior end of the occipital lobe and is known as the earliest and simplest visual processing region. The primary visual area essentially creates a retinotopic map of spatial information attained through visual cues. The location of where information is distributed in V1 is dependant upon where the stimulus is located with respect to the retina and fovea. It is known to process static and dynamic objects and serve in pattern identification. Neurons in V1 provide spatial encoding based on the receptive fields that attain visual information found by the local contrast of imagery. This area is the most studied region for visual studies and it has shown to facilitate in changes in visual orientation, spatial frequencies, color, and play a large role in binocular vision.

The middle temporal (MT) region or V5 is another prominent area in the visual cortex. This area plays a significant role in the perception of motion and unites motion signals to guide in eye movements. Figure 2.9 provides a diagram of the key anatomical regions within the brain described in this section [22].

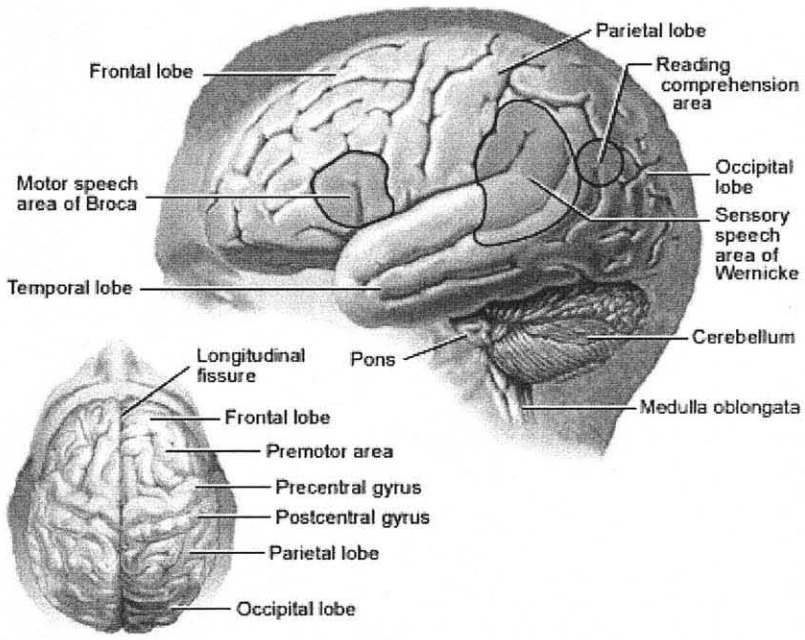

Figure 2.9 Major anatomical and functional regions of the brain.
(Source: http://www.nlm.nih.gov/medlineplus/ency/images/ency/fullsize/1074.jpg)

2.6 BOLD fMRI

Functional and structural MRI vary not only in contrast susceptibility but also in purpose. fMRI is used to identify changes in cortical physiology during a task over time while structural MRI is used to understand the structural anatomy of the brain. Functional MRI attempts to compartmentalize processes to locations within the brain, creating a map. fMRI has allowed for the measurement of confined changes in the cerebral blood flow, volume and oxygenation within particular areas of the brain in response to tasks. Task

induced neural activation results in a vasodilation effect within the vascular system that causes a simultaneous increase in blood flow and a net difference in the level of oxygenation. This is due to an increase in neuronal firing and thus an increase in metabolic activity. Metabolic energy is necessary to nourish and preserve neuronal membrane potentials used for integration of information and signaling. The disparity in oxygenation level creates an increase in the BOLD fMRI signal for all activate regions in the cortex. fMRI studies primarily observe the relationship between these changes and correlate them to a specific stimulus which varies over the presented time. The variable f(t) represents the stimulus, y(t) is the measured fMRI response to the stimulus for each voxel. This can be mathematically represented as (Equation 2.5):

$$y(t) = f(t) \text{ conv } h(t) \tag{2.5}$$

Virtually all fMRI experiments are based upon the measurement of the blood oxygenation level dependant (BOLD) signal. Over a century ago, studies regarding brain function indicated the fundamental concept in fMRI, that deoxygenated hemoglobin exhibits paramagnetic properties while oxygenated hemoglobin is diamagnetic. Additional studies in the early 1980's indicated the variation in magnetic sensitivity due to these different states of hemoglobin which could be quantified using MRI. Along with these results, technological advances of MRI scanners and pulse sequences in the 1990's allowed for the development of fMRI techniques.

During the late 1980's, Seiji Ogawa [23] studied the possibility of observing changes in cortical physiology using MRI. Because the basis of MRI was the abundant hydrogen molecule, it would be very difficult to isolate subtle changes in concentration

corresponding to metabolic variations and interpreting changes in blood flow, and oxygenation of hemoglobin within red blood cells would be a better indicator of activity. Based on prior knowledge that deoxygenation decreases the T2* parameter, Ogawa et al. demonstrated through various in-vitro and in-vivo experiments the ability to generate T2* weighted images by altering blood oxygenation level to vary perceptibility of blood vessels. Ogawa et al. identified this phenomena in which functional changes in activity corresponded to differences in signal on the T2* weighted images as a function of deoxygenated hemoglobin as the blood-oxygenation level dependant (BOLD) contrast. The BOLD contrast was dependant upon the total amount of deoxygenated hemoglobin within a particular region of the brain and the net result between the consumption and supply of oxygen. Although contrast agents have the ability of improving the signal to noise ratio in fMRI images, BOLD response to neural activity (or the hemodynamic response) is primarily used due to its non-invasive nature.

When analyzing the fMRI signal, it is important to understand the nature of the response. In general, the hemodynamic response corresponding to a particular activity does not onset to its maximal activation until approximately 5 seconds into the activity of interest. It is a result of the decrease in deoxygenated hemoglobin due to immediate oxygen extraction. The short-term decrease in the MR signal during the instantaneous onset of neuronal activity before the major positive hemodynamic response component is known as the initial dip. After the completion of the activity, there is a decrease in the responses over an additional 5 to 10 seconds which is followed by a return to a below-baseline state for an extended period of time known as undershoot (Figure 2.10). The predictable nature of the hemodynamic response allows for an improved understanding

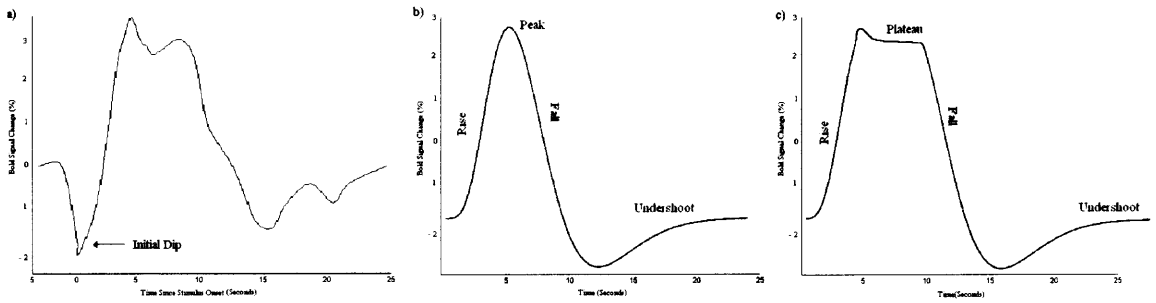

Figure 2.10 (a) Schematic of fMRI BOLD hemodynamic response. (b) Simplified response to a single, short duration stimulus and (c) multiple event stimulus over an extended time (c).

of task induced fMRI signals. The change in the BOLD MR signal for a particular task is known as its time course. The time course of signal intensity in a given voxel typically varies by about 5% about the mean during task activation and 1% during rest. A Fourier transform of a representative resting-state voxel time course shows peaks at the heart and respiratory frequencies. One functional image provides no information about the functionality of the brain and it is only when the functional images are compared that it is possible to interpret results. fMRI enables one to generate images of physiological activity and correlate it to that of neuronal to extract information relating the two.

A key element in fMRI studies involves the comparison of task related changes in the signal to those generated without a task being presented. Three variables are important in quantifying the underlying changes within the fMRI signal: raw SNR (signal to noise ratio), CNR (contrast to noise ratio) and functional SNR. Raw SNR indicates the acquired signal intensity compared to thermal noise produced by the scanner. CNR measures the difference in intensity between tissues in comparison with variability in intensity within the tissues of importance. The functional SNR factor signifies the capability to detect task related changes specifically. As mentioned previously, the raw SNR can be improved linearly with the increase of the magnetic field strength, however

the functional SNR does not improve linearly because it is influenced by additional sources of noise. Although thermal and other hardware related noise do contribute to these factors, they are not as significant as those which are physiologically related. One method often used to improve SNR is signal averaging in which multiple acquisitions are made during a particular task and averaged. Although this may provide an improved SNR, there may be loss of particular task related effects.

Standard fMRI data analysis methods rely upon an estimate of how the fMRI response should result from a particular task. This is done by comparing the voxel time course to a model waveform to determine how well the fMRI data exhibits ideal behavior. Such types of analysis where fMRI data is compared to a pre-determined premise of activity is known as hypothesis-driven analysis. The consequence of using such a method is that assumptions for the hypothesis may not always be valid in situations where the underlying brain activation is unknown. Also for a complex task such as watching a movie, there may not be a specific model waveform applicable to all regions of interest. Although it may be possible to assume a model for the hypothesis, there is no technique to ensure its validity. An alternate approach is data-driven analysis, in which the data is examined without a preconceived model. In this technique, the structure of the data is examined in an attempt to reveal task related activation. Independent component analysis and clustering are two commonly used data-driven techniques in fMRI analysis. Independent component analysis (ICA, described in detail in Section 3.4) assumes that fMRI data can be separated by groups of voxels that vary over time significantly different in activity in comparison to other voxel datasets. The purpose of ICA analysis is to identify groups of voxels based on unique activation

patterns exhibited. ICA allows for analysis without consideration or hypothesis of the idealized activation of the task performed. When implementing clustering analysis, mathematical algorithms are used to identify similarities in the voxel time courses between neighboring groups of voxels to isolate them into segregated clusters. Various studies have utilized this technique to compare clusters of contiguous voxels whose activity was correlated during a task and not during resting conditions. Regions which demonstrated a high co-activation indicate significant functional interconnectivity. Although data-driven analysis techniques do not rely on assumptions on the resulting structure of the hemodynamic response, there are some parameters which constrain this analysis method. Parameters may include the number of independent components or clusters one wants to isolate, in which an increase in parameters will increase the variability and difficulty of interpretation of acquired data. Combining knowledge of the spatial properties of fMRI with data-driven analysis techniques may provide the optimal method in efficiently studying task related functional changes in the brain [22].

Nearly all fMRI studies are based upon the changes in blood oxygenation level over a period of time during a given task. Due to blood oxygenation level changing rapidly after there is an increase in neuronal activity in a particular functional region, fMRI allows for the localization of brain activity with accuracy to the second of activity and millimeters from the origin of activity. Furthermore, due to the intrinsic quality of the blood oxygenation level within the human brain physiology, fMRI is non-invasive and can be repeated multiple times without fear of adverse effects. Because of these many advantages, fMRI has quickly become the primary tool used by thousands in both clinical and research environments to study brain function [22].

CHAPTER 3

INVESTIGATIONAL STUDY

3.1 Subjects

The stimulus was presented to six subjects (4 male, 2 female between ages of 20-30), with no history of neurological disorder or disability. All subjects had normal or corrected to normal vision. Subjects were asked to refrain from moving during the entire session and attempt to comprehend the movie to their best ability. Subjects were given a safety checklist and screening form and it was ensured that they did not have implanted ferrous metal objects such as aneurysm clips and pacemakers within their body. Subjects were also given a brief summary of the general concept of the study. This study was approved by the Institutional Review Board and written consent was obtained from all subjects prior to scanning. All subjects were paid on an hourly basis for their participation.

3.2 Experimental Design

For this study, a 40-minute clip from the motion picture Red Eye (2005) (Wes Craven Production [24]) was used. The selection of this movie (shown in Figure 3.1) was due to

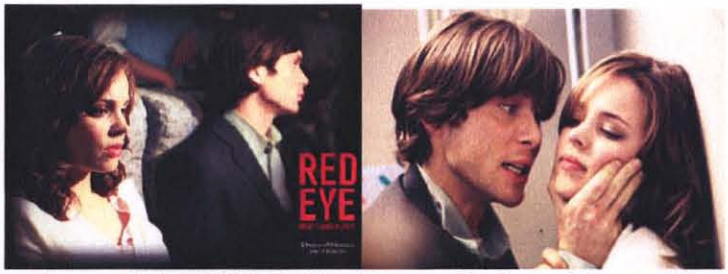

Figure 3.1 Screenshots of the 2005 thriller/drama *Redeye*. Directed by Wes Craven and written by Carl Ellsworth, the plot of the movie involved a hotel manager who is threatened on a routine flight to Miami. She is used as a means to assist in the assassination of a politician. Clips from *Redeye* were shown to subjects during the fMRI scan. (Source: www.allmoviezone.com, www.mustseeflix.com)

its unpredictable and intense emotional nature, as well as the environment presented throughout the film was minimally varying (no sudden changes in scenery). To ensure the novelty of the stimulus, all subjects viewed the movie for the first time during the fMRI study. The entire clip shown took place in an airplane and although the movie had minimal locations that took place outside of the airplane this study excluded these scenes.

The 40-minute stimulus was divided into 8-minute segments followed by a 2-minute "OFF" period, during which a dark blank screen was shown. After the 40-minute presentation, a 10-minute repeat of the initial 40-minute clip was also presented to test for repeatability. Figure 3.2 describes the schematic of the paradigm used for this study.

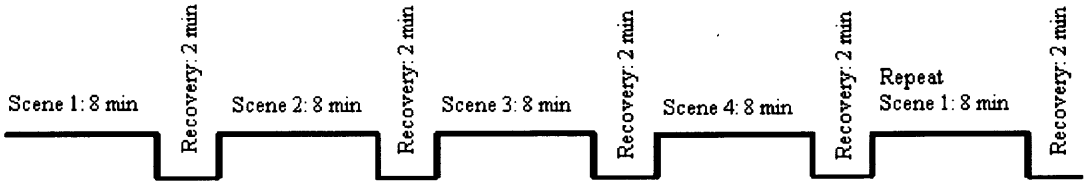

Figure 3.2 Schematic of the paradigm used during the fMRI scan. Four repetitions were shown to the subject that consisted of 8 minutes of stimulus followed by a 2-minute blank screen. Following the total 40-minute scan, the first 10 minutes of the initial scan were shown again to test repeatability.

The stimulus was presented using a LCD projector positioned near the subjects head to a rear-projection screen. Audio was delivered via magnetic resonance compatible pneumatic headphones. The stimulus presentation was triggered simultaneous to the onset of the MRI scanner to ensure that the image acquisition was synchronous to the stimulus presentation for all the subjects.

3.3 fMRI Data Acquisition

All scanning was performed on a Siemens 3T Allegra system (Erlangen, Germany) using a dedicated, non-linear gradient coil. All subjects were positioned supine along the mid-sagital plane. Foam padding was used to minimize head motion. Scanning sessions began with anatomical imaging covering the whole brain. Based on the anatomical images, functional images were produced from the same regions although with lower spatial resolution. Thirty two high-resolution gradient recalled echo images were obtained along the axial slices. The imaging parameters consisted of FOV = 22 cm, Matrix = 256 x 256, TR= 500 msec, TE = 20 msec, where FOV (field of view) is the distance across the image, and matrix size determines the scan resolution. For functional imaging, T2* weighted echo-planar images were obtained from the same location and same number of slices as mentioned during the previous scan. For EPI imaging parameters consisted of FOV = 22 cm, Matrix = 64x64, TR = 2000 msec, TE = 27msec, flip angle = 89 °. This corresponded to a spatial resolution of 3.44 mm x 3.44 mm x 5 mm. After the completion of the functional tasks, high resolution MPRAGE anatomical data sets were collected. MPRAGE imaging parameters consisted of: 80 slices, FOV = 220 mm, Slice thickness = 2 mm, TR = 2000 msec, TE = 4.38 msec, T1 = 900 msec, Flip Angle = 8° (the flip angle of the RF pulse describes how much of the magnetization is converted to MR signal with each excitation), and Matrix = 256 x 256. This corresponded to a spatial resolution of 0.875 mm x 0.875 mm x 1 mm.

Each functional MRI consisted of two tasks, the first task was 40 minutes (1200 images), and the second task was 10 minutes (300 images). The same parameters were used for all the subjects. The sequence of tasks within each scan was also kept the same

for all six subjects. A photograph of the 3T Allegra MRI scanner is given below in Figure 3.3.

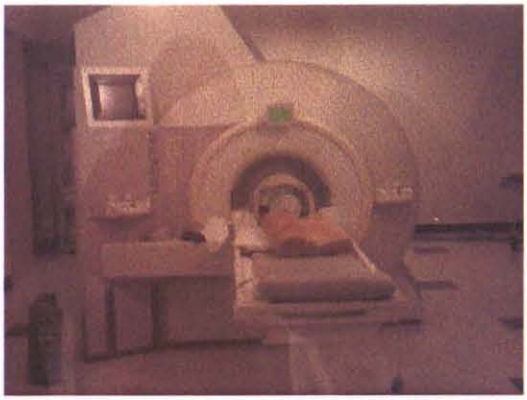

Figure 3.3 The Siemens Allegra 3T MRI scanner located in the Advanced Imaging Center in UMNJ-Newark.

3.4 fMRI Data Analysis

fMRI data preprocessing and analysis were performed using AFNI (Analysis of Functional Neuroimages; Cox, 1995). AFNI [25] allowed for the analysis of the attained fMRI data and the viewing of activation maps for each subject. In addition, AFNI provided various tools to assist in Talairach transformations and statistical analysis on functional datasets. Programs for AFNI could be written in ANSI C format to be run in Linux/Unix workstations.

Due to the lengthy nature of the stimulus, subject motion during scanning was a major concern. Prior to any data analysis, motion detection and correction were performed in AFNI (3dvolvreg) to ensure the accuracy of the data. Data sets were also de-trended to eliminate linear drifts caused by motion, scanner related influences as well as global physiological factors. While a large number of motion corrections methods exist, the 3dvolvreg function was used because a recent comparison of motion registration has shown this method to be as accurate as other methods in addition to being

computationally efficient [26]. In this technique, image registration was done by minimizing the least-squares error between time-series images. This method utilizes the linear nature of the hemodynamic response, which assumes that if stimuli are presented to a subject in close enough intervals the responses overlap and the total fluctuation in the MR signal is a summation of each individual response. The fMRI data can be represented through the following linear model formula in Equation 3.1:

$$y = a_0 + a_1x_1 + a_2x_2 + \ldots + a_nx_n + e \tag{3.1}$$

The linear model formula suggests that the observed data (y) is equivalent to a combination of weighted model factors (x_i). The model factors can be defined as a set of estimated changes in BOLD signal during the particular task. The parameter weights (a_i) indicate the contribution of each factor to the output signal. The error contribution (e) can be minimized by calculating the weight values that will produce a minimized error term. The minimum error term that can be calculated for a given linear system is called the residual. A design matrix is then constructed in coherence with the general linear model determined for the system to observe changes over time. The cost function value summarizes the overall residual error within the system attained from the design matrix and the standard cost function is the least-squares error (used for image registration described previously regarding the 3dvolvreg command) which is the sum of the squared residuals [27].

To facilitate direct comparison between the individual cortices and compensate for variations in anatomy, data sets of each subject were transformed into Talairach coordinates. The Talairach transformation was performed using a process in which the

anterior commisure (AC) and posterior commisure (PC) line of the high resolution anatomical images was initially identified. The longitudinal (inter-hemispheric or mid-sagital) fissure was next aligned to the y-z plane to define the z-axis. After identifying the five landmarks on the high-resolution images, the anatomical images were scaled to the Talairach-Tournox Atlas which allowed for the designation of anatomical regions in the transformed images. An affine transformation was then used to align the two image data sets. Using the Talairach images as a reference, images across subjects could be compared both spatially and temporally.

A data driven temporal correlation method was implemented to detect voxels in the brain mediated by the stimulus. Because this method is described elsewhere in detail it is only briefly described here [28]. This technique assumes that during activation, neighboring voxels have similar temporal characteristics and are clustered together. Thus, every voxel time-course in the brain was correlated to its eight neighboring voxels. The mean correlation coefficient was then calculated on a voxel wise basis for the entire brain. All voxels greater than a value of 0.3 were considered active. Individual activation maps were generated for each subject during each of the two tasks (40 minutes and 10 minutes). Regions that exhibited significant correlation were used for further analysis.

Following the generation of individual activation maps, the Talairach transformed anatomical datasets were averaged and aggregate activation maps were constructed using individual datasets from all subjects. This allowed for the examination of regions that were activate in all of the subjects as well as the degree of correlated spatial activation. A mask was created for the averaged data sets and activated regions exceeding a threshold value of $P = 0.05$ were recognized as statistically significant regions of activation. The

system in which one evaluates whether or not certain conditions exist due to coincidence or significantly is called significance testing. To determine what regions were active in all six subjects the t-test statistic was used. The t-test was used to compare the null hypothesis H_0, that there were different activated regions between subjects and the experimental paradigm did not result in overlapping spatial activation, with the alternate hypothesis H_1 which predicted that the stimulus would result in an overlap of activation in certain regions. The t-test resembles the standard normal distribution however the smaller sample sizes result in more extreme values. To use the t-test it is neccesary to tabulate the means for all data points between the two subject datasets and divide the difference by the overall standard deviation. The t-statistic used is given below in Equation 3.2.

$$t = \frac{\overline{X} - \overline{Y}}{\sqrt{\sigma_x{}^2 + \sigma_y{}^2}} \tag{3.2}$$

The calculated t-statistic is then transformed into a probability value based upon the degrees of freedom or in this case the number of images within the dataset as seen in Figure 3.4. There are two types of corresponding error which may result due to this

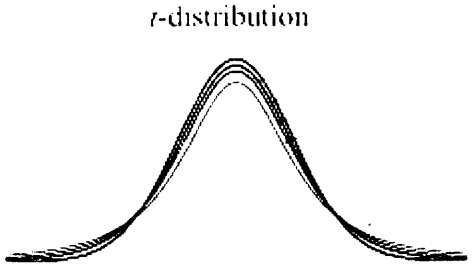

Figure 3.4 t-distribution at various degrees of freedom.
(Source: http://projectile.is.cs.cmu.edu/research/public/talks/ttest/t-test15.gif)

type of statistical testing. The first type, known as Type I error occurs when it is concluded that the null hypothesis is false when it is really true. When considering fMRI this error results when a non-active voxel is considered active (false positive). Type II error results when the null-hypothesis is considered true when it is really false. Regions that demonstated overlap in activation between all six subjects were considered regions of interest (ROIs). ROIs were considered to be homogenous and indivisible during this analysis and each ROI corresponded to an entire anatomical area. ROIs were drawn on high resolution, anatomical MPRAGE images. The ROIs were drawn upon the anatomical images rather than the functional ones due to their high resolution (almost 4 times greater than that of functional images) and better tissue contrast. Althought ROIs were selected based on activation observed in the functional maps, the ROIs were drawn based upon the anatomical extent of the region without consideration to functional activation to provide unbiased estimations of activity within the anatomical ROI. Region of Interest analysis was chosen for this study because it has many advantages over other voxel-wise analysis technques. ROI analysis involves a fewer number of regions than voxel-wise analysis, reducing the number of statistical comparisons and related errors involved. In addition to the reduction in comparisons, ROI analysis averages many voxels within the region and increases the associated signal to noise ratio by assuming that the region is functionally homogeneous.

To estimate the region-specific overlap (RSO) between subjects, the amount of overlap between subjects was quantified through comparison with the anatomical extent of each region. For each ROI, an OR logical operator was first used to find the total number of voxels encompassed within the ROI in the aggregate map of all subjects. An

AND logical operator was then used to determine the number of voxels active in all six subjects within a corresponding ROI. The RSO for each region was then calculated by dividing the number of voxels that overlapped in activation in all six subjects within the ROI by the total number of voxels contained in the respective ROI.

After the ROIs had been selected, the time series from the area enclosed within a recognized ROI were averaged to create one time series dataset per region. Comparison of the voxel time courses from the ROIs were calculated using temporal correlation analysis. Correlation analysis provides a relationship between our measured variables, in our case between the same region in different subjects and between regions within the same subject. Correlation analysis is also useful in identifying changes in signal that are directly associated with task related activities by calculating correlation between predicted and measured responses. The characteristics of the hemodynamic responses allows for the prediction of task induced changes in the fMRI signal for active voxels. The correlation coefficient indicates the strength of the relationship between the variables and a coefficient value of 1 indicates a linear relationship between the measurements and a value of 0 indicates no relationship. For data measurements from a sample of subjects, the correlation coefficient, denoted r, is calculated as follows (Equation 3.3):

$$r = \frac{Cov(X,Y)}{\sqrt{Var(X)Var(Y)}} \tag{3.3}$$

where the variances and covariances of X and Y are defined by Equations 3.4, 3.5, and 3.6:

$$Var(X) = \frac{\sum (X - \bar{X})^2}{n-1} \tag{3.4}$$

$$Var(Y) = \frac{\sum (Y - \bar{Y})^2}{n-1} \tag{3.5}$$

$$Cov(X,Y) = \frac{\sum (X - \bar{X})(Y - \bar{Y})}{n-1} \tag{3.6}$$

Correlation analysis using fMRI data was first introduced by Bandettini et al. [4,22] and has since become a significant tool for the analysis of fMRI data. The time series datasets from each particular region were correlated both inter-subject (same region, different subject) and inter-regionally (same subject, different region). There are two prominent techniques in the approach to inter-subject statistical analysis with fMRI data. The approach utilized in this study is known as fixed-effects analysis. Fixed-effects analysis assumes that the effects resulting from the experimental design are constant among participants and any differences between the datasets attained from subjects is due to random noise. The alternative approach to inter-subject analysis is random-effects analysis, which suggests that there is a variable effect on each subject resulting from the experiment. Thus, from each subjects correlation matrix the temporal correlation between any two regions could be determined. Similarily, from the correlation matrix for a particlar region temporal correlation between any two subjects could be determined. All correlation analysis was performed on MATLAB software.

For all regions that displayed significant RSO, the relationship between RSO and temporal correlation between subjects were compared. Because Hasson et al. [1] had reported an average spatial overlap across the cortical surface between subjects to be 29%

± 10 SD, only regions that demonstrated RSO greater than 19% between all six subjects were used. For every region that exhibited RSO greater than 19%, the corresponding mean temporal correlation was determined and regression performed to determine the relationship between RSO and the average regional temporal correlation between subjects as the linear trend line and R^2 values were computed.

The observed fMRI signal can be considered as a linear mixture of various "signal" sources originating from task induced signal changes, other physiological signals such as the heart rate and respiration rate, and some motion parameters. Most data analysis methods determine "where" the sources occur but not "what" the sources giving rise to the signal changes are (i.e., task-induced, cardiac, respiratory). Independent Component Analysis (ICA) which is a popular "blind-source separation" technique was applied to the analysis of fMRI data from each subject [27, 29, 30]. It is often used to solve the "cocktail party" problem in which multiple people are speaking simultaneously and the source of each of the voices us unknown. If it is assumed that there are a number of microphones located at various locations in the room (equal to or grater than the number of voices present in the room), using ICA on the resulting signal from each microphone which contains a mixture of signals will separate the individual signal based on each speaker. The purpose of ICA is to identify all independent variables within a set of data and understand which underlying components are most dominant. The general model of a signal that can be separated using ICA describes a signal based upon a linear combination (described previously) of signals from independent sources. The model can be written mathematically as follows (Equation 3.7):

$$x_i(t) = a_{i1}\, s_1(t) + a_{i2}\, s_2(t) + \ldots + a_{iN}\, s_N(t) \quad \text{for } i = 1, \ldots\ldots, N \quad \text{and in matrix form} \quad \begin{bmatrix} x_1(t) \\ x_2(t) \\ \cdot \\ \cdot \\ x_n(t) \end{bmatrix} = A \begin{bmatrix} s_1(t) \\ s_2(t) \\ \cdot \\ \cdot \\ s_n(t) \end{bmatrix} \tag{3.7}$$

ICA is used to find the mixing matrix, A from which the independent signals s may be found using an inversion technique. Voxel time courses from each of the regions were obtained and decomposed into a number of independent components. Each of the significant ICA components were then correlated with each of the active regions to determine significant correlation between them. Thus, the number of significant components affecting the inter-regional connectivity could be quantified.

3.5 Results

Motion was not found to be significant in any of the runs for each of the subjects. The mean motion component for the x, y, and z axis was found to be -0.201, 0.634, and -0.199 mm, respectively.

Spatial activation patterns corresponding to the stimulus were identified using the regional homogeneity method [28]. A threshold corresponding to a significance value of $p < 0.005$ was used to determine all voxels mediated by the stimulus. All voxels greater than the threshold were considered active and their locations were noted for further analysis. Table 3.1 provides a list of the ROIs and their Talairach Transformation coordinates.

Table 3.1 Regions of Interest: Talairach Coordinates, Region-Specific Overlap and Inter-Subject Temporal Correlation

Region		Region-Specific Overlap	Average Temporal Correlation	Talairach Coordinates		
				x	y	z
ROI 1	Culmen (L)	57.5%	0.4917 ± 0.1614	20	46	-16
ROI 2	Fusiform Gyrus (R)	5.9%	0.2731 ± 0.1429	-40	48	-16
ROI 3	Middle Temporal Gyrus (R)	67.1%	0.2506 ± 0.1178	-52	39	0
ROI 4	Middle Occipital Gyrus (R)	15.9%	0.1947 ± 0.1351	-35	83	9
ROI 5	Inferior Frontal Gyrus (L)	3.6%	0.2567 ± 0.1621	44	-24	2
ROI 6	Inferior Temporal Gyrus (R)	29.3%	0.1860 ± 0.1225	-56	39	-13
ROI 7	Superior Temporal Gyrus (R)	18.6%	0.3385 ± 0.2411	-51	17	0
ROI 8	Superior Temporal Gyrus (L)	17.3%	0.3242 ± 0.2172	51	17	0
ROI 9	Posterior Cingulate (L)	69.0%	0.2464 ± 0.1526	10	54	14
ROI 10	Posterior Cingulate (R)	76.0%	0.1385 ± 0.1363	-10	54	14
ROI 11	Cuneus (R)	63.8%	0.1067 ± 0.0776	-13	83	18
ROI 12	Anterior Cingulate (L)	31.9%	0.1595 ± 0.1665	8	-32	7
ROI 13	Precentral Gyrus (L)	11.9%	0.4467 ± 0.1602	44	8	38
ROI 14	Middle Occipital Gyrus (L)	80.7%	0.3660 ± 0.2144	35	83	9
ROI 15	Middle Temporal Gyrus (L)	6.7%	0.3501 ± 0.2201	52	39	0
ROI 16	Postcentral Gyrus (L)	4.2%	0.2299 ± 0.1657	43	25	43
ROI 17	Middle Frontal Gyrus (R)	8.5%	0.1680 ± 0.1909	-9	-24	35
ROI 18	Supramarginal Gyrus (R)	48.5%	0.3139 ± 0.1596	-51	48	31
ROI 19	Precuneus (L)	23.6%	0.1673 ± 0.1142	14	61	41
ROI 20	Insula (R)	21.4%	0.2049 ± 0.1628	-39	7	9
ROI 21	Precentral Gyrus (R)	16.4%	0.2582 ± 0.2666	-44	8	38

In each of the subjects, a number of distinct anatomical regions were found to be active. These regions included the middle temporal gyrus, occipital gyrus, posterior cingulate, cuneus and other audio-visual regions. Spatial activation maps constructed for two subjects are provided in Figure 3.5.

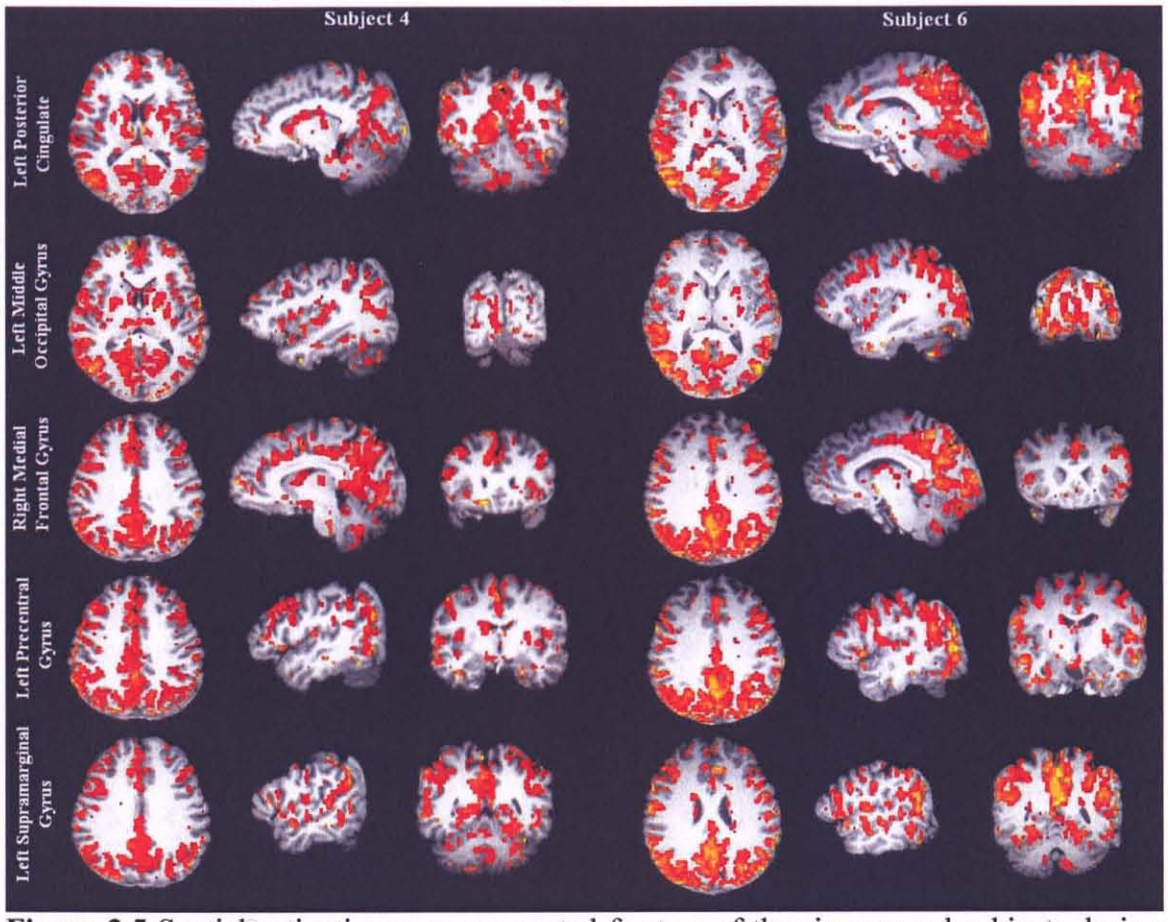

Figure 3.5 Spatial activation maps generated for two of the six scanned subjects during the 40-minute scan. Activation in the left posterior cingulate, left middle occipital gyrus, right medial frontal gyrus, left precentral gyrus and left supramarginal gyrus are shown. Noticeable similarities between subjects existed for corresponding regions as can be seen in the figure.

RSO between all six subjects was found to be quite significant in many regions including left posterior cingulate, right middle temporal gyrus, left middle occipital gyrus. About 69% of the left posterior cingulate and 76% of the right posterior cingulate demonstrated overlap. The right middle temporal gyrus showed 67.1% RSO and the left middle occipital gyrus exhibited an 80.7% region-specific overlap. Other areas such as the left culmen and right cuneus indicated 57.5% and 63.8% RSO, respectively. Details of the extent of RSO between subjects are given in Table 3.1 by region.

Although the spatial activation maps obtained from the 40-minute scan and 10-minute scan had significant overlap between them, there were several differences. It was seen that the spatial activation maps from the 40-minute stimulus had considerably less number of false positives (random voxels that were not part of a larger cluster consisting of 5 or more voxels). The spatial extent of noteworthy (observed in all six subjects) activation (dark red regions in Figure 3.6) obtained from the 40-minute scan was also found to be greater than the 10-minute scan, as can be seen in Figure 3.6. During the 40-minute scan, the spatial extent of activation across all six subjects corresponding to the stimuli covered 19.43% of the cortical surface, while the 10-minute scan resulted in activation that extended across 12.7% of the cortical surface.

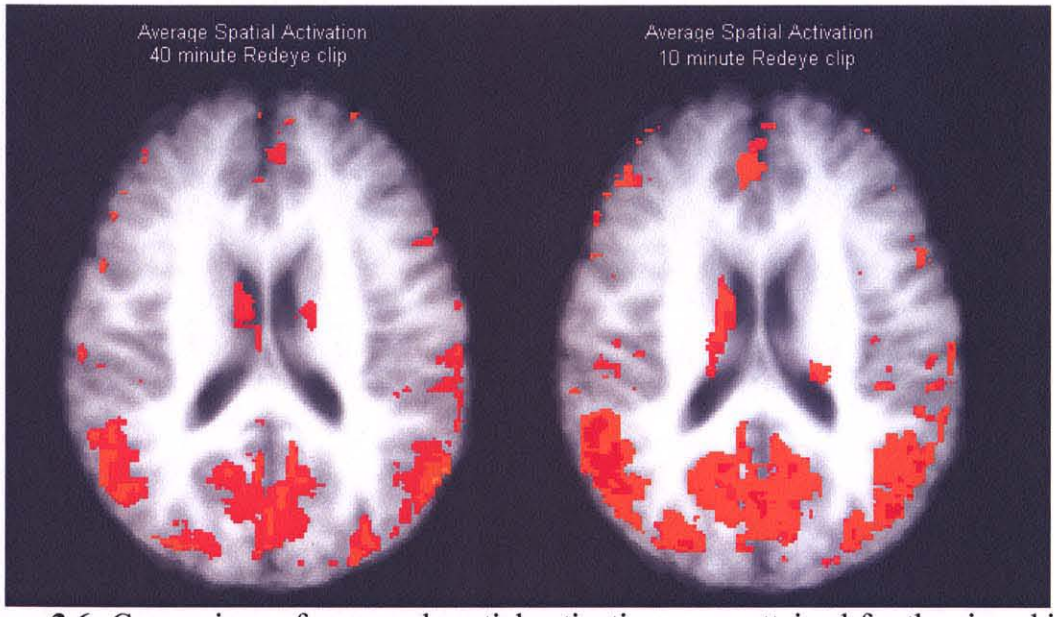

Figure 3.6 Comparison of averaged spatial activation maps attained for the six subjects scanned in this study during the initial 40-minute and repeated 10-minute scans. Observable differences can be seen between the two brains as activation was considerably more robust during the initial viewing.

Inter-regional correlation was computed pair wise using the averaged voxel time courses from each of the ROIs. Temporal correlation analysis was performed between each of the ROIs for each of the subjects. Significant temporal correlation was observed between a number of the activated ROIs. Two significant groups of regions that shared activation patterns were observed during inter-regional correlation. The first group included the left culmen, right inferior temporal gyrus, left superior temporal gyrus, precuneus, right insula, right/left precentral gyrus, left middle temporal gyrus, left inferior frontal gyrus, and right superior temporal gyrus. The mean correlation coefficient between these regions was about 0.664±0.048. The second group which demonstrated similar activity included the right fusiform gyrus, right middle occipital gyrus, right cuneus, left middle occipital gyrus, and right/left posterior cingulate. The mean correlation coefficient between the regions was found to be 0.703±0.070. The left post central gyrus showed correlation to both groups and the right middle temporal gyrus, left anterior cingulate, and right medial frontal gyrus showed correlation to neither group. For each of the subjects the first five independent components accounted for more than 95% of the variance of the voxel time-course chosen from the activated ROIs.

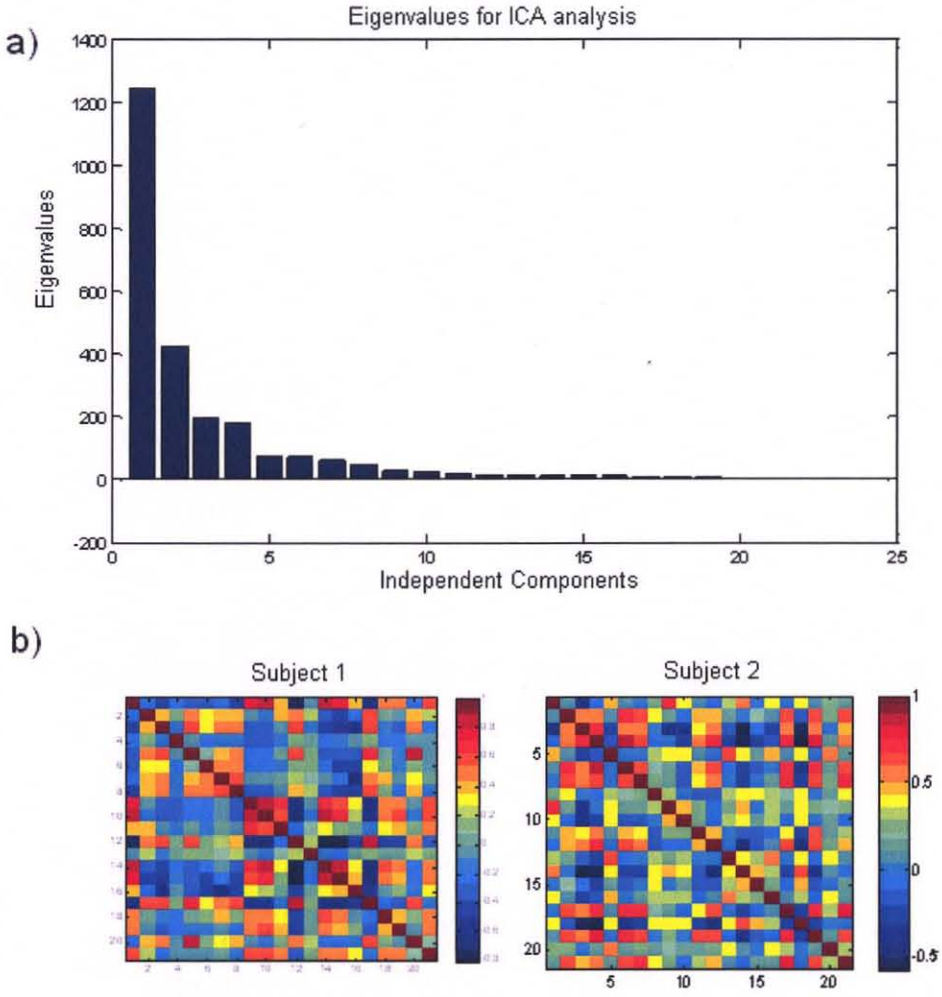

Figure 3.7 Inter-region analysis within subjects during 40-minute initial viewing. a) Components identified through Independent Component Analysis (ICA) for one of the scanned subjects. b) Inter-region correlation matrices for two subjects.

Eigenvalues attained through ICA are shown in Figure 3.7a. Further, the first component accounted for at least 50% of the total variance in all six subjects. Each of these components was then correlated with an average voxel time series from each of the ROI. The dominant independent component had a correlation coefficient greater than 0.4 in 15 of the 21 ROIs. Those regions that had dominant correlation with component one include the left culmen, right inferior temporal gyrus, left posterior cingulate, left anterior

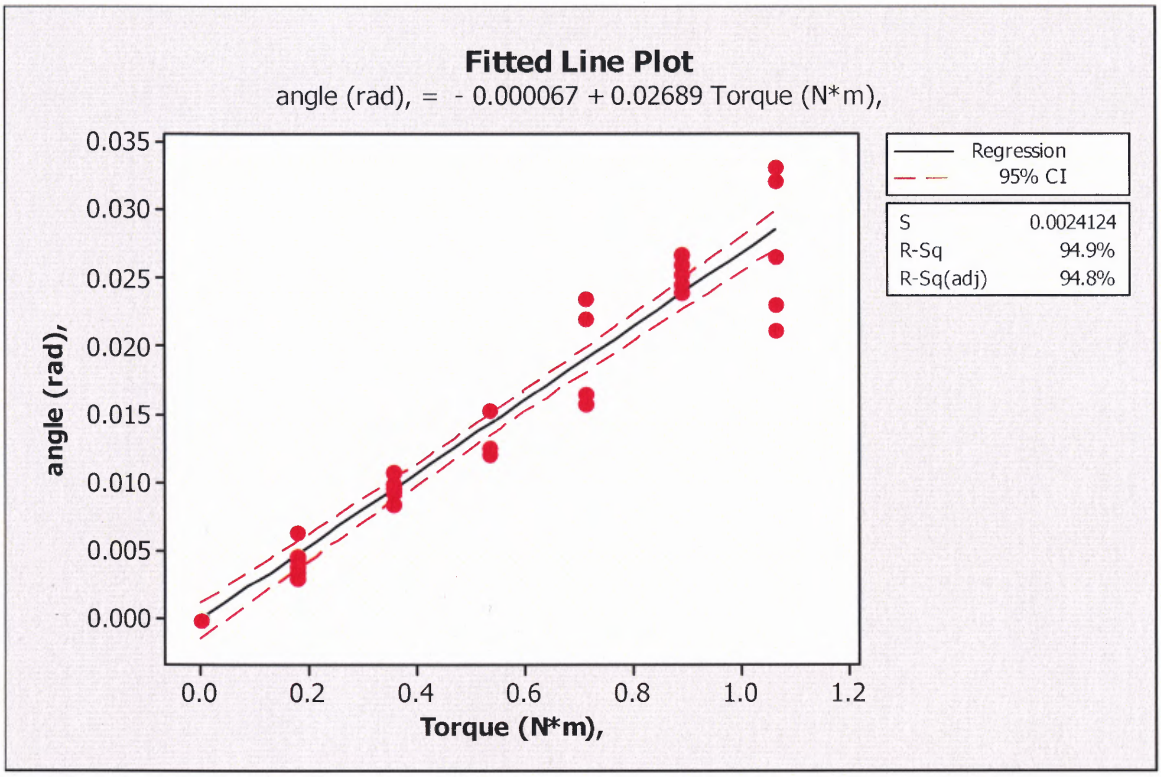

Figure 5.13 Linear regression of equilibrium-point angle vs. applied initial torque trials for subject 4.

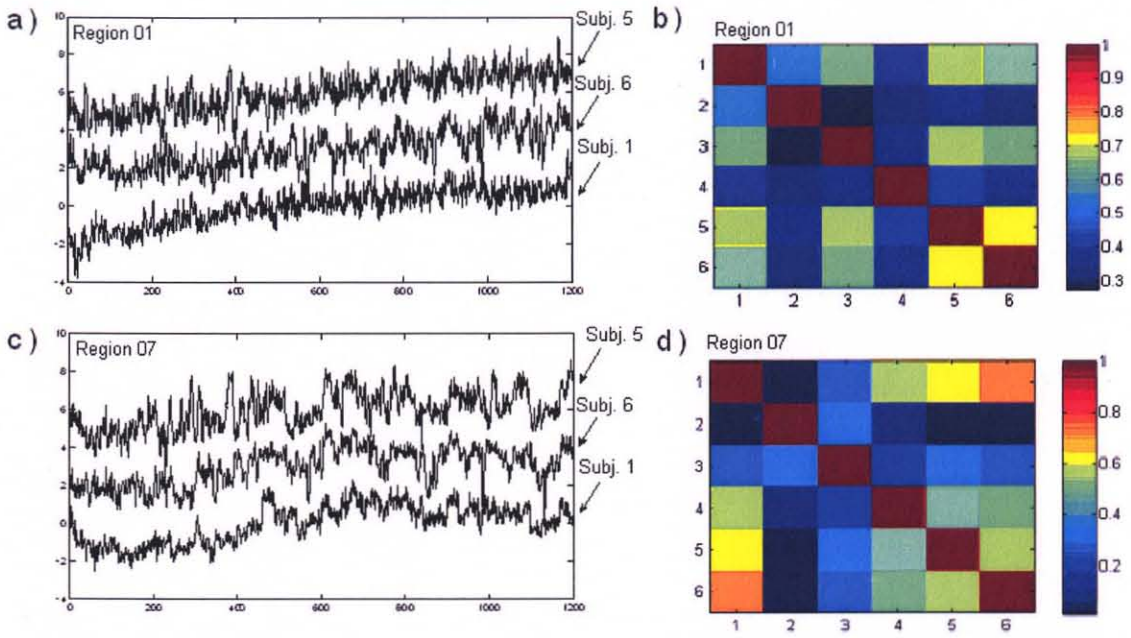

Figure 3.8 Inter-subject analysis during 40-minute initial viewing. a) Time series data from the left culmen (Region 01) for three of the six scanned subjects. b) Inter-subject correlation matrix within the six scanned subjects for Region 01. c) Time series data from the right superior temporal gyrus (Region 07) for three of the six scanned subjects. d) Inter-subject correlation matrix within the six scanned subjects for Region 07. Similarities in the time series data can be seen between the three subjects. Correlation analyses suggest correlation coefficients between subjects during the 40 minute viewing to exceed 0. 7.

A regression between RSO from different regions that exhibited inter-subject overlap within the ROI greater than 19% and their corresponding temporal correlation values was plotted. The correlation coefficient and the corresponding R^2 value were found to be 0.487 and 0.238 respectively. This indicates a relatively linear relationship between RSO between subjects and their subsequent mean inter-subject temporal correlation.

3.6 Discussion

Although this study was similar to the one conducted by Hasson et al [1] and Bartels and Zeki [17], there were several differences in its design and implementation to control various parameters. To minimize the effects of newly introduced visual objects, cues and distractions, the entire movie clip presented occurred within an airplane. All the subjects scanned were familiar with the environment having flown atleast one international (> 10 hours) flight within the last year. The movie also focused around two primary characters, eliminating additional diversions. Recently, Furman et al. [31] have shown that subjects can remember many events in a presented movie months after watching it. To minimize these kinds of memory effects, all subjects who participated in the study were asked explicitly if they had viewed the movie previously. Only those who had not seen the movie, read reviews about the movie and were unfamiliar with the plot and actors in the movie were selected as subjects for this study. This brings up the inquiry "why would we expect variations in activation between subjects when we are presenting an identical stimulus under such control?" Numerous factors contribute to the variability in inter-subject activity. A major factor is the individual physiology of each subject which determines the morphology of the hemodynamic response. Furthermore, when using a simple stimulus the responses from subjects would be similar however, a movie is quite a complicated stimulus. The stimulus contained a visual, auditory, language and emotional component and because subjects were told to casually view the movie without fixation to any component in particular they were able to fixate on any attribute or combination of them which they desired to. Responses were also dependant on each subject's bias and personal experience and further, how each individual felt about a particular scene,

character, or situation. This variability in personal opinion during such a dynamic and integrated stimulus would create significant variability during the relatively uncontrolled and natural scenario presented through the stimulus.

Spatial activation maps provoked by the stimulus (watching movie) were observed in each of the subjects. Similar spatial activation patterns were observed in all 6 subjects in a number of distinct anatomical regions including the culmen, fusiform gyrus, middle temporal gyrus, middle occipital gyrus, inferior frontal gyrus, right insula, superior temporal gyrus, posterior cingulate, anterior cingulate, cuneus, precentral gyrus, postcentral gyrus, medial frontal gyrus, and parts of the supramarginal gyrus. This was consistent with the study conducted by Hasson et al. [1] in which synchronization extended beyond audiovisual sensory cortex. Additional regions which were found both in the study performed by Hasson et al. as well as our study include entire superior temporal (STS) and lateral sulcus (LS), retrosplenial gyrus, secondary somatosensory regions in the post-central sulcus, multimodal areas in the inferior frontal gyrus and parts of the limbic system in the cingulate gyrus. Several regions involved with higher order functions were identified in addition to the basic visual and auditory regions [32, 33]. Higher order cognitive functions are those which are considered to be of the mental operations associated with humans rather than non-human creatures. These regions are considered to be those pertaining to consciousness, executive function, abstract reasoning, and autobiographical memory. Many regions with very specific function were also active for example, the fusiform gyrus [34, 35] which was active in all six subjects has been linked to face recognition. Regions related to visual, sensory integration, and processing of spatial information that were active due to the stimulus in all subjects

included the culmen, middle occipital gyrus, cuneus, and retrosplenial gyrus. Active regions that play a role in motor function included the precentral gyrus, postcentral gyrus, and medial frontal gyrus. In addition to the audiovisual component, there was a contextual component present in the stimulus presented which mediated activation in regions such as the middle temporal gyrus, superior temporal gyrus, lateral sulcus, and inferior frontal gyrus which are known to demonstrate functionality during language related tasks and phonological processing. Many regions that have been shown to exhibit cognitive function were also active between subjects during the stimulus. One such region was the insula, which is responsible for the feeling of basic emotions such as anger, fear, sadness and happiness was also responsive. The anterior cingulate, a region responsible for the execution of tasks, learning, problem solving, motivation and anticipation, and emotional responses demonstrated considerable activity. Spatial activation was also observed in the supramarginal gyrus and pre-frontal areas, regions that have been linked to cognitive and motor related function, which were not seen in the previously mentioned study by Hasson et al. [1].

Significant temporal correlation was found between several subjects across numerous corresponding regions in this study. Temporal correlation as high as 0.8 were observed across several subjects during the initial 40-minute viewing. This suggests that specific regions of the brain such as the culmen, precentral gyrus, middle occipital gyrus, and middle temporal gyrus process information in a similar manner over several minutes in response to identical stimuli. These previously described regions in which correlations were observed are thought to be involved in audiovisual information processing as well as the integration of somatosensory information [36]. This high temporal correlation

would be very unlikely be due to any drifts, respiratory, or cardiac signals, since in addition to the respiration rate being different between subjects, it is quite improbable that the signals even with the same frequency would be in phase. After filtering the data to remove artifacts originating from respiration, no significant differences between the original and the filtered data could be identified. Further, correlation between subjects for corresponding regions increased following filtering (although not significantly). The previously mentioned study conducted by Bartels et al. [17] indicated a mean temporal correlation between the 4 ROIs to be 0.32 ± 0.104. The mean temporal correlation value for this study between the 21 ROIs (unfiltered data) was 0.261 ± 0.166.

As a measure of reliability, the first ten minutes of the forty minute *Redeye* scanning was repeated at the end of the session. Temporal correlation was performed between the first ten minutes of the forty minute scan for each region with corresponding region from the ten minute scan. In a few subjects temporal correlation over 0.3 were observed in the unfiltered time series data. This suggests that brain activation patterns are quite similar when observing identical stimuli however, the somewhat low correlation may indicate that there is a habituation effect that occurs between the first and second presentation, as the novelty of the stimulus diminishes.

In this study, various methodologies were used to detect and quantify spatial and temporal correlation within and across subjects. A number of methods are presented including regional homogeneity and independent component analysis, all of which can be used to detect and localize similarities in activation patterns. Although each of the methods are unique approaches to analyzing these types of paradigms, all were used together to re-validate results.

CHAPTER 4

CONCLUSION AND FUTURE WORK

In conclusion, results indicated a considerable overlap spatially and temporally between six subjects during the presentation of the movie stimulus. Although there were no instructions given to the subjects regarding fixation on the stimulus, there was a high similarity in the regions that were active during the movie clip. During the 40 minute clip it was observed that 19.43% of the cortical surface was active between all six subjects, consistent with the results attained by Hasson et al. [1]. Regions which exhibited this activation pattern were not only found in functional areas related to audio-visual tasks, but areas of higher cognition as well. Temporal correlation was performed on all 21 ROIs between the six subjects and unfiltered time-course datasets indicated a mean correlation value of 0.261 ± 0.166 with regions such as the culmen demonstrating correlation as high as 0.4917 ± 0.1614 between subjects. Inter-regional correlation within subjects isolated two major components which represented the activation patterns for all 21 ROIs, illustrating significant brain connectivity during the task. This study utilized the innovative technique of performing inter-subject and inter-region brain mapping during a natural task which contained a contextual component in addition to auditory and visual cues. This allowed for the understanding of similarities in processing mechanisms between individuals during less constrained conditions.

This investigation provides a basic framework for future studies and numerous applications in neuro-imaging. A few of the ideas suggested for further use are provided. Understanding the similarities in brain functionality during a complex stimulus within a certain population will allow for the comparison in processing between different

demographics. One for example, can compare the activation patterns between young and old populations during identical stimulus. It is also possible to utilize these techniques to compare various lingual backgrounds and observe the significance of language comprehension during complicated tasks. Inter-subject correlation methods can be used to understand the changes that occur in processing mechanisms within clinical patients suffering from various conditions such as Schizophrenia, ADHD, Autism, Alzheimer's disease, comatose patients and other neurological function related disorders. Underlying processes for working memory can also be examined. As suggested by Furman et al., [31] memories of a previously viewed movie can last an extended period of time. How memory effects activation patterns between subjects can be tested by comparing those who have viewed a particular sequence at varying durations. The investigation performed in this study enforced certain constraints in the number of characters present in scenes as well as the environment in which the movie took place, however further studies may remove these restrictions and implement others such as using attentional effects as a regressor to identify changes in connectivity maps when constraints are altered.

Recently, multivariate analyses have been used to train neural networks to classify patterns of fMRI activation evoked by the visual presentation of various categories of objects. Additional applications may include implementation of neural networks in "brain reading" algorithms for complicated stimuli [37]. Currently, this classification by neural networks has only been performed by small datasets corresponding to simple stimuli, however understanding the fMRI activation patterns elicited by complicated stimuli will allow for the creation of more intricate neural networks.

The study conducted incorporated both cognitive neuroscience and signal processing strategies to identify the similarities in cortical functionality during natural vision. This investigation extended upon studies previously performed to carefully examine the extent of this synchronization both spatially and temporally. The use of a movie clip, rather than a psychophysically controlled stimulus which elicited responses in a specified area, allowed us to activate a number of regions corresponding to a variety of functions in a single duration. Using a range of analytical techniques, consisting of regional homogeneity, independent component analysis, regression analysis and inter-subject and inter-regional correlation, it was possible to identify distinct functional regions which displayed comparable activity. This method of mediating activity in numerous cortical regions through an individual stimulus may prove to be useful in studying similarities of brain function, not only in normal subjects but also in comparison of clinical patients, presenting assistance in developing effective rehabilitation strategies.

REFERENCES

[1] Hasson U, Nir Y, Levy I, Fuhrmann G, Malach R. (2004) Intersubject synchronization of cortical activity during natural vision. Science. Mar 12;303(5664):1634-1640.

[2] Belliveau JW, Kennedy DN, McKinstry RC, et al. (1991) Functional mapping of the human visual cortex by magnetic resonance imaging. Science Nov 1:254(5032) :716 -719

[3] Ogawa S, Tank DW, Menon R, Ellermann JM, Kim SG, Merkle H, Ugurbil K. (1992) Intrinsic signal changes accompanying sensory stimulation: functional brain mapping with magnetic resonance imaging. Proc Natl Acad Sci USA. Jul 1:89(13):5951-5955.

[4] Bandettini PA, Wong EC, Hinks RS, Tikofsky RS, Hyde JS. (1992) Time course EPI of human brain function during task activation. Magn Reson Med. Jun:25(2):390-397

[5] Kwong KK, Belliveau JW, Chesler DA, Goldberg IE, Weiskoff RM, Poncelet BP, Kennedy DN, Hoppel BE, Cohen MS, Turner R, Rosen B, Brady TJ (1992) Dynamic magnetic resonance imaging of human brain activity during primary sensory stimulation. Proc Natl Acad Sci USA June 12:89(12):5675-5679.

[6] Binder JR, Rao SM, Hammeke TA, Yetkin FZ, Jesmanowicz A, Bandettini PA, Wong EC, Estkowski LD, Goldstein MD, Haughton VM. (1994) Functional magnetic resonance imaging of human auditory cortex. Ann Neurol. Jun:35(6):662-672.

[7] Rao SM, Binder JR, Hammeke TA, Bandettini PA, Bobholz JA, Frost JA, Myklebust BM, Jacobson RD, Hyde JS. (1995) Somatotopic mapping of the human primary motor cortex with functional magnetic resonance imaging. Neurology. May:45(5):919-924.

[8] Tootell RB, Reppas JB, Kwong KK, Malach R, Born RT, Brady TJ, Rosen BR, Belliveau JW. (1995) Functional analysis of human MT and related visual cortical areas using magnetic resonance imaging. J Neurosci. 1995 Apr;15(4):3215-30.

[9] DeYoe EA, Carman GJ, Bandettini P, Glickman S, Wieser J, Cox R, Miller D, Neitz J. (1996) Mapping striate and extrastriate visual areas in human cerebral cortex. Proc Natl Acad Sci USA. Mar 19:93(6):2382-2386.

[10] Petrella JR, Shah LM, Harris KM, Friedman AH, George TM, Sampson JH, Pekala JS, Voyvodic JT. (2006) Preoperative Functional MR Imaging Localization of

Language and Motor Areas: Effect on Therapeutic Decision Making in Patients with Potentially Resectable Tumors. Radiology;240:793-802

[11] Hou BL, Bradbury M, Peck KK, Petrovich NM, Gutin PH, Holodny AI. (2006) Effect of brain tumor neovasculature defined by rCBV on BOLD fMRI activation volume in the primary motor cortex. NeuroImage Aug 15;32(2):489-97

[12] Quarles CC, Krouwer HG, Rand SD, Schmainda KM.(2005) Improving the reliability of obtaining tumor hemodynamic parameters in the presence of contrast agent extravasation. Magn Reson Med. Jun;53(6):1307-16

[13] Quarles CC, Krouwer HG, Rand SD, Schmainda KM.(2005) Dexamethasone normalizes brain tumor hemodynamics as indicated by dynamic susceptibility contrast MRI perfusion parameters. Technol Cancer Res Treat. Jun;4(3):245-9

[14] Schiff ND, Rodriguez-Moreno D, Kamal A, Kim KH, Giacino JT, Plum F, Hirsch J. (2005) fMRI reveals large-scale network activation in minimally conscious patients. Neurology. Feb 8;64(3):514-23

[15] Schiff ND, Ribary U, Moreno DR, Beattie B, Kronberg E, Blasberg R, Giacino J, McCagg C, Fins JJ, Llinás R, Plum F. (2002) Residual cerebral activity and behavioural fragments can remain in the persistently vegetative brain. Brain. Jun;125(Pt 6):1210-34

[16] Schiff ND, Plum F, Rezai AR. (2002) Developing prosthetics to treat cognitive disabilities resulting from acquired brain injuries. Neurol Res. Mar;24(2):116-24

[17] Bartels A, Zeki S. (2004) Functional brain mapping during free viewing of natural scenes. Hum Brain Mapp. Feb:21(2):75-85.

[18] Bartels A, Zeki S. (2005) Brain dynamics during natural viewing conditions--a new guide for mapping connectivity in vivo. NeuroImage. Jan 15:24(2):339-349.

[19] Malinen S, Hlushchuk Y, Hari R. (2007) Towards natural stimulation in fMRI--issues of data analysis. NeuroImage. Mar;35(1):131-9

[20] DeYoe EA, Bandettini P, Neitz J, Miller D, Winans P. (1994) Functional magnetic resonance imaging (FMRI) of the human brain. J Neurosci Methods. Oct:54(2):171-187.

[21] Bushberg JT, Seibert JA, Leidholdt EM, Boone JM The Essential Physics of Medical Imaging Philadelphia, PA, 2002.

[22] Huettel SA, Song AW, McCarthy G, Functional Magnetic Resonance Imaging. Sunderland, MA, 2004.

[23] Ogawa S, Lee TM, Nayak AS, Glynn P (1990) Oxygenation-sensitive contrast in magnetic-resonance image of rodent brain at high magnetic-fields. Magn Reson Med 14 :68-78.

[24] Redeye. Dir. Wes Craven. Perf. Rachel McAdams, Cillian Murphy. 2005. DVD. Dreamworks SKG.

[25] Cox RW (1996), AFNI: software for analysis and visualization of functional magnetic resonance neuroimages, Comput. Biomed. Res. 29 pp. 162-173.

[26] Oakes TR, Johnstone T, Ores Walsh KS, Greischar LL, Alexander AL, Fox AS, Davidson RJ. (2005) Comparison of fMRI motion correction software tools. Neuroimage. Nov 15;28(3):529-43. Epub 2005 Aug 15.

[27] Biswal BB, Ulmer JL. (1999) Blind source separation of multiple signal sources of fMRI data sets using independent component analysis. J Comput Assist Tomogr. Mar-Apr:23(2):265-71

[28] Zang Y, Jiang T, Lu Y, He Y , Tian L. (2004) Regional homogeneity approach to fMRI data analysis. NeuroImage, May: 22(1): 394-400.

[29] McKeown MJ, Jung TP, Makeig S, Brown G, Kindermann SS, Lee TW, Sejnowski TJ. (1998) Spatially independent activity patterns in functional MRI data during the stroop color-naming task. Proc Natl Acad Sci USA. Feb 3:95(3):803-10.

[30] Calhoun VD, Adali T, Pearlson GD, Pekar JJ. (2001) Spatial and temporal independent component analysis of functional MRI data containing a pair of task-related waveforms. Hum Brain Mapp. May:13(1):43-53.

[31] Furman O, Dorfman N, Hasson U, Davachi L, Dudai Y (2007) They saw a movie: Long-term memory for an extended audiovisual narrative. Learn. Mem. **14**: 457-467

[32] Wilson SM, Molnar-Szakacs I, Iacoboni M (2007) Beyond Superior Temporal Cortex: Intersubject Correlations in Narrative Speech Comprehension. Cereb Cortex. May 15

[33] Gates L, Yoon MG (2005) Distinct and shared cortical regions of the human brain activated by pictorial depictions versus verbal descriptions: an fMRI study, NeuroImage 24 473- 486

[34] Gauthier I, Tarr MJ, Moylan J, Skudlarski P, Gore JC, Anden AW (2000) The fusiform "face area" is part of a network that processes faces at the individual level, J. Cogn. Neurosci. 12: 295-504.

[35] Kourtzi Z, Kanwisher N (2000) Cortical regions involved in perceiving object shape, J. Neurosci. 20: 3310

[36] Ganis G, Thompson WL, Kosslyn SM (2004) Brain areas underlying visual mental imagery and visual perception: an fMRI study, Cognitive Brain Research 20: 226-241

[37] Cox DD, Savoy RL.(2003) Functional magnetic resonance imaging (fMRI) "brain reading": detecting and classifying distributed patterns of fMRI activity in human visual cortex. Neuroimage. 2003 Jun;19:261-70.